Materials Today Nano 4 (2018) 1–16

Contents lists available at ScienceDirect

Materials Today Nano

journal homepage: https://www.evise.com/profile/#/MTNANO/login

Status, promises, and challenges of nanocomposite solid-state electrolytes for safe and high performance lithium batteries

J. Wan [a, 1], J. Xie [a, 1], D.G. Mackanic [b], W. Burke [a], Z. Bao [b], Y. Cui [a, c, *]

[a] Department of Materials Science and Engineering, Stanford University, CA, 94305, USA
[b] Department of Chemical Engineering, Stanford University, CA, 94305, USA
[c] Stanford Institute for Materials and Energy Sciences, SLAC National Accelerator Laboratory, 2575 Sand Hill Road, Menlo Park, CA, 94025, USA

ARTICLE INFO

Article history:
Received 14 October 2018
Received in revised form
7 December 2018
Accepted 8 December 2018
Available online 21 December 2018

Keywords:
Composite solid-state electrolyte
Active and passive filler
Aligned interface
Physical and chemical stability
Processability

ABSTRACT

All-solid-state Li batteries (ASSLBs) are well recognized as potentially high energy density, safe systems for future energy storage. The development of solid-state electrolytes is one of the most crucial steps for ASSLBs. Nanocomposite solid-state electrolytes (CSSEs)—which contain both polymer electrolytes and nanoscale inorganic fillers (such as inorganic solid electrolyte filler)—have attracted tremendous interest with their good processability, flexibility, and reasonable ionic conductivity. In this review article, we will discuss the recent progress, design principles, and challenges of CSSEs for ASSLBs.

© 2019 Elsevier Ltd. All rights reserved.

1. Introduction

Li-ion batteries exist ubiquitously in modern society, finding roles in areas such as portable electronics, electrical vehicles, and grid-scale energy storage [1–5]. Commonly used, commercialized Li-ion batteries are comprised of a Li transition metal oxide cathode and graphite anode, separated by a nanoporous separator and organic liquid electrolyte [6–8]. However, the growing demands for higher energy density surpass the limit of state-of-the-art Li-ion chemistry (250 Wh/kg), and thus, other chemistries that allow for higher energy density are urgently needed [9–18]. With this movement toward higher energy density, safety issues for Li-ion batteries become even more critical, considering the serious accidents already associated with the current Li-ion technology [19]. The rise of metallic lithium as the 'ultimate' anode material for Li batteries brings with it both opportunities and challenges for their operation [20–26]. Dendritic Li growths—which are commonly formed during plating and stripping—can potentially pierce the separator, leading to short circuit and safety hazards.

A revolutionary Li battery design would potentially solve the aforementioned issues, enabling high energy density and safe Li batteries. Instead of using a liquid, flammable organic electrolyte with a separator, a Li-ion conductive solid-state electrolyte (SSE) could be placed in between the cathode and anode of the Li battery [27–35]. A mechanically rigid, non-flammable SSE film would ideally suppress the dendritic Li metal formation, leading to safe operation of high-capacity Li batteries. In addition, solid/solid interfaces are expected to have slower side reactions, which would lead to improved coulombic efficiency and cycle life for all-solid-state Li batteries (ASSLBs).

Currently, both inorganic and organic materials are known to conduct Li ions. Thus, the study of SSEs is grouped into three categories: glasses/ceramics [28], polymers [19], and their hybrids [36]. The main advantages of glass/ceramic SSEs are their high Li-ion conductivity (10^{-4}–10^{-2} S/cm) at ambient temperature, mechanical rigidity, and lack of flammability. However, the brittle nature of thin glass/ceramic films and the fact that Li grows along the grain boundaries of these SSEs may hinder their application as SSE in ASSLBs [37,38]. Pure polymer SSEs are flexible and have high processability, but their low intrinsic Li-ion conductivity (10^{-8}–10^{-5} S/cm) at ambient temperature and soft nature limit their utilization for ASSLBs [39]. Thus, a system that combines the advantages of the aforementioned two SSE categories while

* Corresponding author.
E-mail address: yicui@stanford.edu (Y. Cui).
[1] These authors contributed equally to this work.

https://doi.org/10.1016/j.mtnano.2018.12.003
2588-8420/© 2019 Elsevier Ltd. All rights reserved.

avoiding their weaknesses is needed for ASSLBs. Fortunately, sophisticated designs for hybrid systems of inorganic/organic solid electrolytes show promise in addressing the problem. We will discuss the development of nanoscale composite solid-state electrolytes (CSSEs) in five aspects, namely ionic conductivity, physical stability, chemical stability, processability, and advanced characterizations in the later sections, as shown in Fig. 1.

2. Improving the Li-ion conductivity in CSSE

The discovery of an ionically (alkali metal ion) conductive solid polymer—a poly(ethylene oxide) (PEO) salt complex—was first made by Fenton et al. [40] and Wright [41] and suggested by Armand et al. for use as a solid electrolyte for electrochemical devices [42,43]. Since then, a variety of polymer electrolytes with high Li-ion conductivity have been reported, such as poly(acrylonitrile) (PAN) [44,45], poly(methyl methacrylate) (PMMA) [46,47], poly(-vinyl chloride) (PVC) [48], poly(ethylene carbonate) (PEC) [49], and poly(vinylidene fluoride) (PVDF) [50]. However, most of these polymer systems containing significant amount of liquid additive and the resulting systems are therefore more properly known as gel electrolytes. This practice mainly stems from the fact that the aforementioned dry polymers display limited to negligible dry Li ionic conductivity and thus can hardly compete with the PEO system in an all-solid case [36]. PEO has a high dielectric constant and solvates Li ions easily, and the motion of its -(CH2-CH_2-O)$_n$-segments and the breaking/formation of interchain/intrachain lithium-oxygen coordination bonds are mainly what induce the Li-ion movement in the complex. This mechanism implies that amorphous PEO with higher chain flexibility should offer greater Li-ion conductivity, and so the majority of literature works concentrate on inhibiting the crystallinity of the PEO polymer matrix. Despite this, a few reports suggest that crystalline PEO is capable of obtaining higher conductivity than its amorphous counterpart [51,52]. The glass transition temperature (T_g) of a polymer is a critical measurement of its degree of chain motion because polymer chains are able to move at temperatures above the T_g of a system. Thus, it is possible to enhance the ionic conductivities of a polymer solid electrolyte by lowering its T_g [53]. It is similarly important to pursue a high lithium transference number to ensure effective Li-ion transport and uniform, non-dendritic Li deposition [54].

Various strategies, such as the addition of fillers, plasticizers, or block copolymer crosslinking have been demonstrated to improve the ionic conductivity, Li-ion transference number, and/or mechanical properties of solid polymer electrolytes (SPEs) [53,55–58]. Of particular importance is the addition of ceramic fillers as it holds a number of advantages. The addition of ceramic fillers can disrupt the crystallinity of polymers and provide ionic pathways along the polymer/ceramic interface, leading to higher ionic conductivity. If these fillers are also intrinsically Li-ion conductive, additional ionic pathways are provided through the ceramic fillers themselves. Ceramic fillers, in general, have also been shown to improve the mechanical strength, temperature/voltage stability range, and lithium-ion transference number of polymer solid-state electrolytes without compromising their processability and flexibility. As the addition of ceramic fillers affords a unique and diverse set of benefits, in this section, we will be delving into the myriad attempts at adding ceramic fillers to CSSEs to improve their performance. Note that the ionic conductivity of a CSSE depends on a variety of factors, including the type of polymer used, the molecular weight of the polymer, the ratio of polymer repeating units (i.e. ethylene oxide) to Li ions, the type of Li salt used, whether the polymer is linear or cross-linked, and the addition of waxy or liquid plasticizers. As a result, although it is difficult to compare the ionic conductivities from different references, some general structure-property relationships can still be concluded from the existing literature.

2.1. Addition of fillers with random structures to CSSE

2.1.1. Addition of passive fillers to CSSE

Passive fillers used to improve the performance of solid polymer electrolytes include the canonical ceramic oxides and more exotic materials such as graphene oxide [59], clays [60], and metal-organic frameworks (MOFs) [61]. Poorly Li-ion conductive

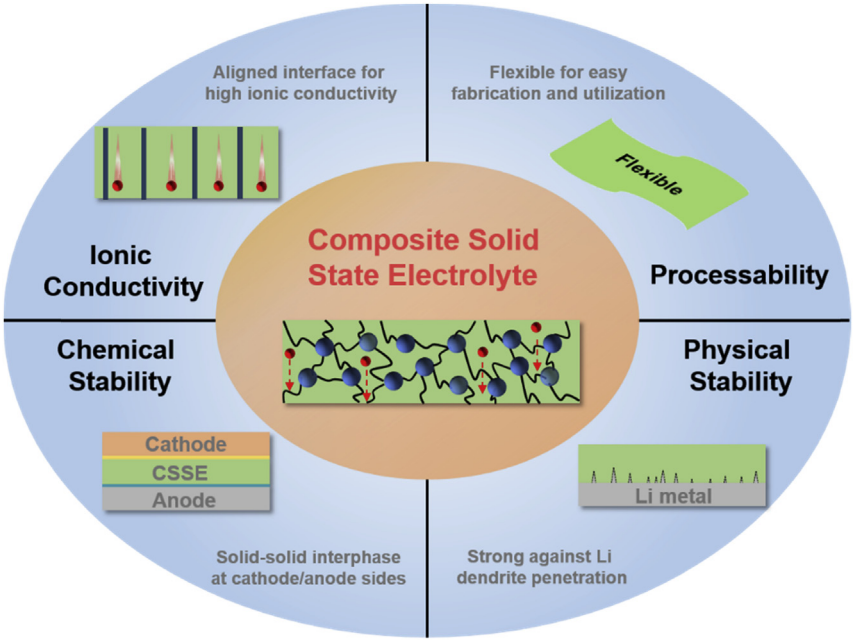

Fig. 1. Schematic of the promises and challenges of composite solid-state electrolyte (CSSE) for Li batteries.

materials as passive fillers were first introduced to solid polymer electrolytes to enhance their mechanical and interfacial properties (Fig. 2a) [62]. However, no ionic conductivity increase was observed as the added particles are large (40 μm) [62,63]. In the late 1980s, researchers reported that the addition of fine ceramic fillers (diameter ranging from submicron to a few microns) enhanced the ionic conductivity of CSSEs [39,64]. The addition of small particles increases the volume fraction of the amorphous phase of the polymer/salt, leading to a corresponding increase in ionic conductivity. In 1998, Croce et al. [65] first reported that the addition of nanoscale ceramic particles (5.8–13 nm) in PEO/$LiClO_4$ electrolyte enhanced the ionic conductivity of the polymer electrolyte over three orders of magnitude at ambient temperature (2×10^{-5} S/cm at 31 °C, Fig. 2b). The high ionic conductivity resulted from the large surface area of the nanoparticles, which locally prevented the recrystallization of polymer chains in the cooling process (from above 60 °C, the melting temperature of PEO), and from the Lewis acid–type surface of the nanoparticles [66]. A high transference number of 0.6 is also achieved with this type of CSSE, whereas the transference number of pure PEO/$LiClO_4$ is as low as 0.2–0.3. Wieczorek et al. [67] reported a detailed study on the Lewis acid surface effect of CSSEs, in which it was found that the Lewis acid center can form complexes with anions, helping the dissociation of the Li salt and plasticizing the system. The Lewis acid center also can interact with polymer chains and thus stiffen the CSSE. However, the *ex situ* addition of particles down to a few nanometers often leads to the agglomeration of nanoparticles [68]. Such agglomerations do not allow for the full utilization of the aforementioned large surface area and lead to residual crystallized polymer regions. To overcome this problem, Lin et al. [69] reported the *in situ* synthesis of SiO_2 nanoparticles with PEO/$LiClO_4$ (Fig. 2c). This method successfully demonstrated the effect of monodispersed SiO_2 nanoparticles in the PEO/$LiClO_4$ matrix, with the nanoparticles obtaining both chemical and mechanical bonding with the PEO chains. This design shows enhanced ionic conductivity (4.4×10^{-5} S/cm at 31 °C) compared to an ex situ addition of SiO_2 nanoparticles with the same diameter and concentration [69].

A network of 1D passive nanowires provides a better percolation Li-ion conducting pathway than what is achieved with 0D nanoparticles. Liu et al. [70] report the addition of nanowires that do not conduct Li into a PAN/$LiCLO_4$ complex, which shows higher Li-ionic conductivity (1.07×10^{-5} S/cm at 30 °C) than the nanoparticle scenario (2.89×10^{-6} S/cm at 30 °C). The same group further introduced a lightweight, large-surface-area 3D structure—SiO_2 aerogel—as filler for CSSE [71] (Fig. 2d–f). This novel design, when combined with cross-linked PEO/Lithium bis(trifluoromethanesulfonyl)imide (LiTFSI), demonstrated excellent mechanical properties (modulus of 0.43 GPa, hardness of 170 MPa) and ionic conductivity (6×10^{-4} S/cm at 30 °C), even though a plasticizer of succinonitrile was added.

2.1.2. *Addition of active fillers to CSSE*

Unlike passive ceramic fillers, active ceramic fillers exhibit high intrinsic Li ionic conductivity. Typical active fillers include garnet-structured $Li_7La_3Zr_2O_{12}$ (LLZO) and perovskite-structured $Li_{3x}La_{2/3-x}\square_{1/3-2x}TiO_3$ (LLTO) [28]. The attempts of adding active fillers for CSSE are slightly behind compared to passive fillers [39]. Because both components of such a CSSE would provide Li-ion conductivity, the overall ionic conductivity is expected to be higher than that of a CSSE with passive additives. The early attempts of adding active Li_3N showed promise in terms of increasing the ionic conductivity, but a large portion (>90%) of the active material was needed to

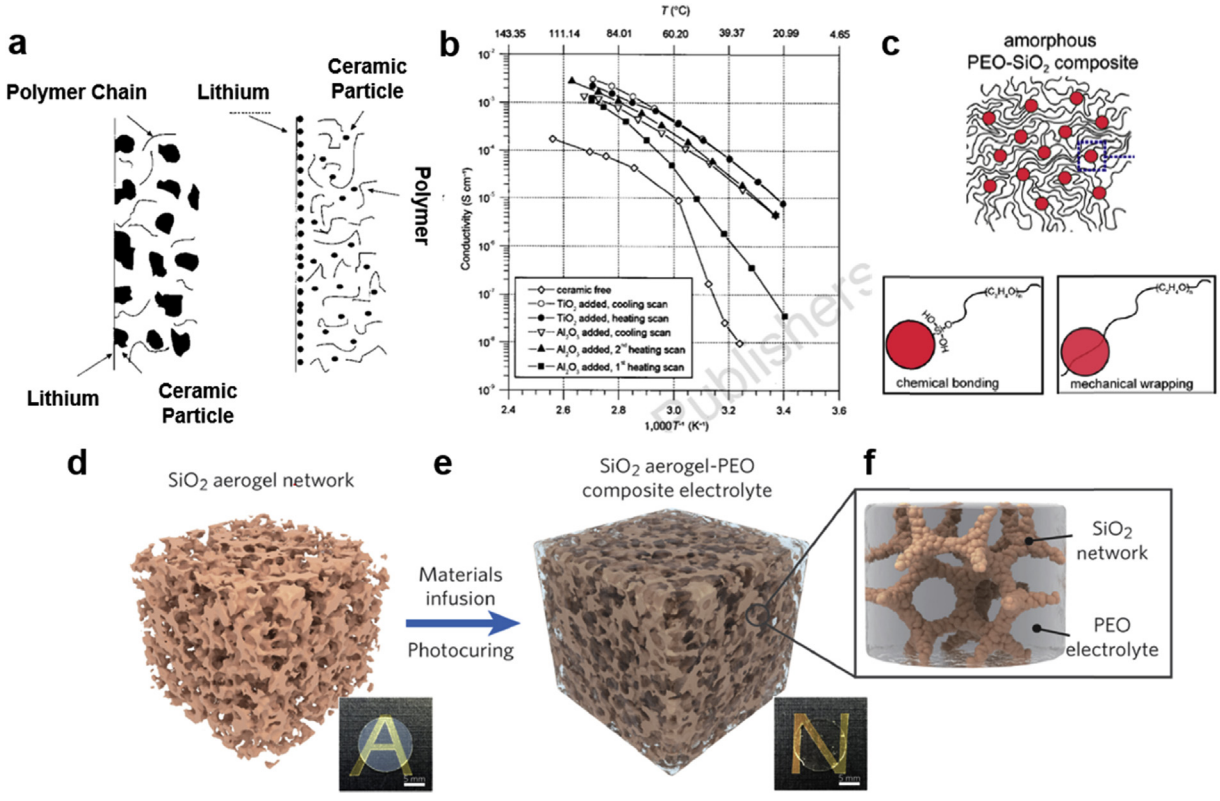

Fig. 2. Adding passive fillers in polymer electrolyte for CSSEs. (a) Schematic of CSSE with ceramic particle fillers at various sizes. Reproduced with permission from Elsevier. (b) Ionic conductivity plot of ceramic-free polymer electrolytes vs. oxide nanoparticle–added CSSEs. Reproduced with permission from Nature publishing group. (c) Schematic of in situ synthesized, monodispersed SiO_2 fillers in PEO/LiClO4 complex CSSE. Reproduced with permission from American Chemical Society. (d) Schematic of SiO_2 aerogel-PEO CSSE. Reproduced with permission from John Wiley and Sons. CSSE, composite solid-state electrolyte; PEO, poly(ethylene oxide).

maintain this higher ionic conductivity (1×10^{-4} S/cm at 30 °C) [39,72]. Plocharski et al. [155] reported that the addition of (Na) super ionic conductor (NASICON)-type active fillers in PEO/NaI produces effects similar to those achieved with the addition of alumina powders—i.e. an enhanced ionic conductivity of 1×10^{-5} S/cm at room temperature. More recently, Zhang et al. [73] reported a CSSE composed of PEO/LiTFSI and Li-ion–conducting Al-doped $Li_{6.75}La_3Zr_{1.75}Ta_{0.25}O_{12}$ (LLZTO) particles with moderate Li-ion conductivity (1.12×10^{-5} S/cm at 25 °C, Fig. 3a and b). This CSSE obtained a high transference number of 0.58, much higher than is seen in regular polymer electrolytes and common liquid electrolytes, and is comparable to CSSEs with passive fillers. This CSSE shows excellent flexibility and good resistance to Li dendrites. With the addition of more LLZTO in a polymer electrolyte matrix, a transition from 'ceramic-in-polymer' to 'polymer-in-ceramic' takes place, as is demonstrated by Chen et al. [74] The highest ionic conductivity (1.17×10^{-4} S/cm at 30 °C) is achieved with 10 wt% of LLZTO particles. When the LLZTO loading reaches 85 wt%, its mixture with PEO and Poly(ethylene glycol) (PEG) demonstrates excellent flexibility as a film (Fig. 3h and i), which can survive bending and twisting tests. A similar work carried out by Pandian et al. [75] reported a CSSE with high ceramic concentration (greater than 60 vol%), which showed an excellent Li^+ transference number of 0.79. Other active additives also reportedly enhance the performance of CSSEs. Wang et al. [76] reported that the addition of active $Li_{1.3}Al_{0.3}Ti_{1.7}(PO_4)_3$ (LATP) nanoparticles (diameter of 65 nm) in PEO/LiClO4 results in a record high ionic conductivity of 1.7×10^{-4} S/cm at 20 °C, surpassing that of passive TiO_2 nanoparticle (diameter 21 nm) and SiO_2 nanoparticle (diameter 250 nm) systems. Highly ionically conductive SSE particles, such as $Li_{10}GeP_2S_{12}$, can also be incorporated in polymer electrolyte matrices for CSSEs [77]. Ionic conductivities of 1.21×10^{-3} S/cm at 80 °C and 1.18×10^{-5} S/cm at 25 °C can be achieved with the incorporation of only 1% of active additive, a significant improvement over pure PEO-LiTFSI polymer electrolyte (7.98×10^{-4} S/cm at 80 °C and 6.16×10^{-6} S/cm at 25 °C).

1D fibrous filler additives to polymer electrolytes are expected to have a better effect than those of 0D particles because the ionic percolation pathway at the polymer/ceramic interphase in a 1D system is more efficient (Fig. 4a) [78]. Liu et al. [79] demonstrated a high ionic conductivity of 2×10^{-4} S/cm at 25 °C with the addition of 15 wt% of LLTO nanowires in PAN/$LiClO_4$ complex (SEM image shown in Fig. 4b). The enhanced ionic conductivity is attributed to the surface Li vacancy of the LLTO nanowires. Similar results were also reported by Yang et al. [80] by adding 5 wt% of Ta-doped LLZO nanowires to a PAN/$LiClO_4$ complex, achieving an ionic conductivity of 1.5×10^{-4} S/cm at 20 °C. Fu et al. [81] further extended the 1D fibrous fillers to a 3D interconnected fibrous network (Fig. 4c), where the 3D LLZO network was synthesized through an electrospinning/calcination process, as shown in Fig. 4d. The as-synthesized CSSE film shows decent flexibility with a high ionic conductivity of 2.5×10^{-4} S/cm at 25 °C. The same group later utilized a textile template–assisted synthesis procedure with an LLZO textile to form a LLZO/PEO/LiTFSI CSSE (Fig. 4e and f). The ionic conductivity for this study was reported to be 2.7×10^{-5} S/cm at 25 °C [82].

2.2. Addition of fillers with ordered structures to CSSE

2.2.1. Addition of discontinuously aligned fillers

In the aforementioned discussions, all of the CSSEs demonstrated isotropic Li-ion conductivity because the fillers were randomly oriented in the polymer matrix. The discontinuous and tortuous nature of these polymer/filler interfaces (Fig. 5a and b) suggests that the Li ionic conductivity of these CSSEs has not been maximized. It is also worth mentioning that, when stretched, a pure polymer/Li salt complex shows enhanced Li ionic conductivity along its stretched direction [83,84]. Therefore, an aligned polymer/filler interface with fast Li-ion transport properties needs to be developed for high ionic conductivity (Fig. 5c). Kitajima et al. [85] introduce magnetically aligned 2D montmorillonite (MMT) ceramic plates in PEO/$LiClO_4$ to form such an aligned CSSE. Fig. 5d–f shows the 2D Wide-angle X-ray scattering (WAX) patterns and schematics of random, horizontally aligned and vertically aligned MMT in a cross-linked PEO matrix, respectively [85]. At 30 °C, the vertically aligned CSSE shows higher ionic conductivity than both

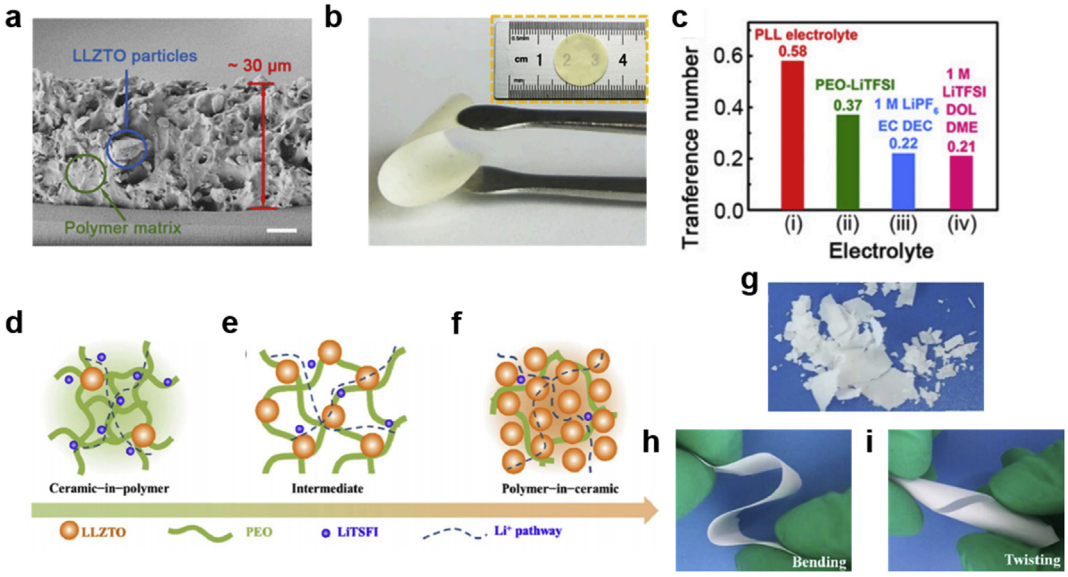

Fig. 3. Adding active fillers to polymer electrolyte for CSSEs. (a) SEM image and (b) photo images of LLZTO particle/PEO CSSE. Reproduced with permission from National Academy of Sciences, USA. (c) Li-ion transference numbers of various electrolyte systems. (d–f) Schematic images of LLZTO particle/PEO CSSE at various concentrations. (g) Photo image of LLZTO particle/PEO CSSE (without PEG). (h–i) Photo images of LLZTO particle/PEO CSSE with PEG (the weight ratio of PEO:LLZTO:PEG is 10:85:5). Reproduced with permission from Elsevier. CSSE, composite solid-state electrolyte; LLZTO, $Li_{6.75}La_3Zr_{1.75}Ta_{0.25}O_{12}$; PEO, poly(ethylene oxide); SEM, scanning electron microscopy; DOL, 1,3-dioxolane; DME, dimethoxyethane; EC, ethylene carbonate; DEC, diethyl carbonate; PLL, (PEO)–lithium bis(trifluoromethylsulphonyl)imide (LiTFSI)-LLZTO.

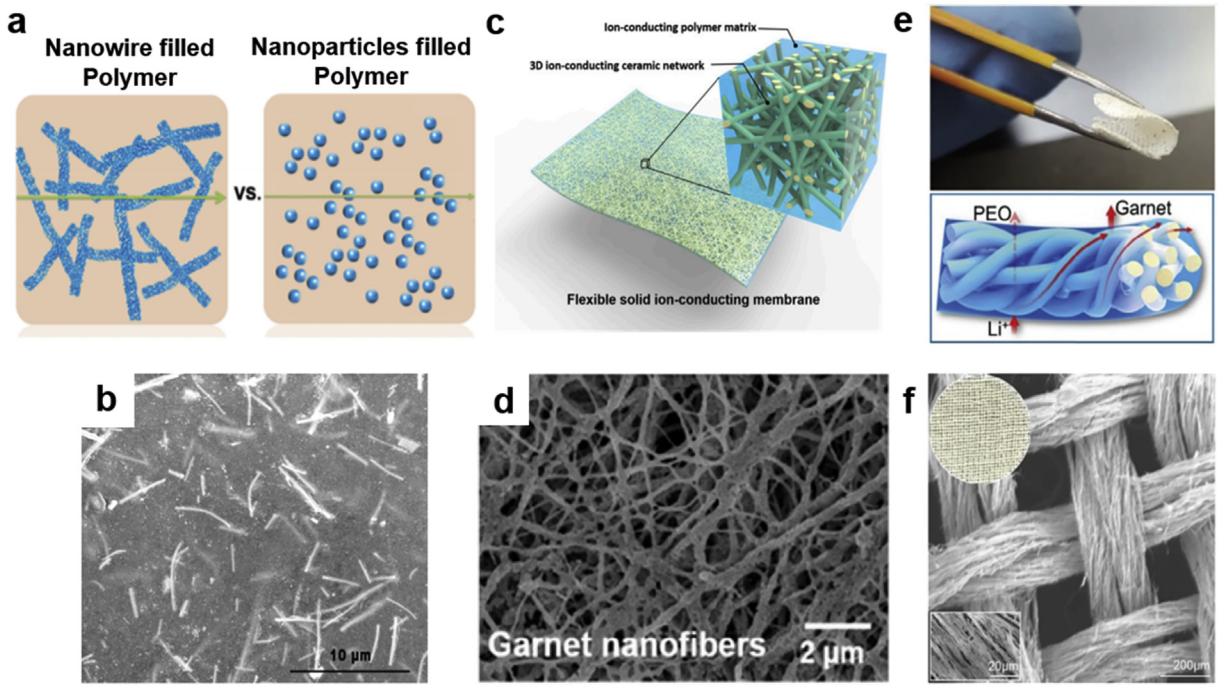

Fig. 4. Combining polymer electrolyte with random networks of active ceramic filler for CSSEs. (a–b) Schematic and SEM images of LLTO nanowires in a PAN/$LiClO_4$ system. Reproduced with permission from American Chemical Society. (c–d) Schematic and SEM images of 3D LLZO network in PEO/LiTFSI system. Reproduced with permission from National Academy of Sciences, USA. (e–f) Schematic and SEM image of LLZO woven textile in PEO/LiTFSI system. Reproduced with permission from Elsevier. CSSE, composite solid-state electrolyte; LLTO, $Li_{3x}La_{2/3-x}\square_{1/3-2x}TiO_3$; LLZO, $Li_7La_3Zr_2O_{12}$; PAN, poly(acrylonitrile); PEO, poly(ethylene oxide); SEM, scanning electron microscopy.

pure polymer electrolyte and random/horizontally aligned CSSE at a wide range of filler concentrations (5 wt% to 20 wt%, Fig. 5h). However, the authors show that at 20 wt% of MMT in the CSSE, the vertically aligned CSSE only shows a higher conductivity than the other CSSEs under 60 °C (Fig. 5g). Although this demonstrates the enhancement effect of vertical alignment for ionic conductivity, the overall ionic conductivity of the vertically aligned MMT CSSE (1.2×10^{-5} S/cm at 30 °C) is not high when compared to other CSSEs.

2.2.2. Addition of continuously aligned fillers

To demonstrate the enhancement effect of continuously aligned fillers, Liu et al. measured the ionic conductivity of LLTO nanofibers with PAN/$LiClO_4$ CSSE at different orientations (0°, 45°, 90°, random, Fig. 6a–d). The continuously aligned LLTO nanowires show the highest conductivity among all orientations and two orders of magnitude enhancement compared with filler-free polymer electrolyte in a wide temperature range (Fig. 6e) [86]. This work shows the importance of a continuous interface for aligned CSSEs although the ionic conductivity measurement was performed by horizontally oriented interdigital electrodes. In fact, these structures with anisotropic properties have also been widely utilized in energy applications [87–89]. Other works by Zhang et al. [90] and Zhai et al. [91] demonstrated that passive anodized aluminum oxide (AAO) (Fig. 6f and g) and active LATP templates provide vertically aligned interfaces with enhanced ionic conductivity compared to their filler-free counterparts. The highest ionic conductivities achieved by solid AAO/PEO/LiTFSI and LATP/PEO/$LiClO_4$ are 1.79×10^{-4} S/cm at 25 °C and 5.2×10^{-5} S/cm at 25 °C, respectively. Although the structures can be potentially used for real battery applications, neither of the works demonstrated the utilization of these CSSEs with full-cell configurations, which is potentially due to difficulties in fabricating it with the CSSEs. It is worth noting that unlike magnetic field–assisted alignment, the in situ electrical field–assisted alignment (with active fillers) is able to create a (quasi)continuous interface (Fig. 6i–j) and leads to a greater enhancement of ionic conductivity than CSSE with randomly orientated fillers [92]. An extreme extension of this case would be changing the (quasi)continuous interface to a continuous, one-particle-thick layer of ion-conducting ceramic in thin polymer membrane, which is demonstrated by Aetukuri et al. [37], although the authors used a Li-ion–insulating polymer membrane and the ionic conductivity is not directly reported. From the aforementioned discussions, we conclude that a less tortuous, continuous network of active inorganic/organic interfaces would benefit the ionic conductivity of CSSEs. This could be achieved through the creation of a continuous 3D inorganic additive scaffold or well-aligned inorganic network.

2.3. Transference number of CSSE

The transference number is defined as the fraction of the total ionic current carried in an electrolyte by a given ionic species, such as lithium ions (t_{Li+}) or its anions (t_{anion}) [93]. In polymer electrolytes, the lithium-ion transference number is generally (with some exceptions) very low (t_{Li+}<0.3) due to the coexistence of dissociated, mobile anions in the system [36,94,95]. The low t_{Li+} leads to the buildup of a large concentration gradient inside batteries upon operation and is detrimental to cell performance [96]. However, the addition of functional inorganic additives in CSSEs partially immobilizes these anions due to surface Lewis acid-base interactions and thus allows CSSEs to have an ion transference number superior to that of SPEs [59,66,97].

3. Physical stability of CSSE

Physical stability is a key measurement of a composite polymer electrolyte's prospects for application within batteries. Possessing the highest specific capacity and lowest electrochemical potential, lithium metal has long been considered the most promising anode

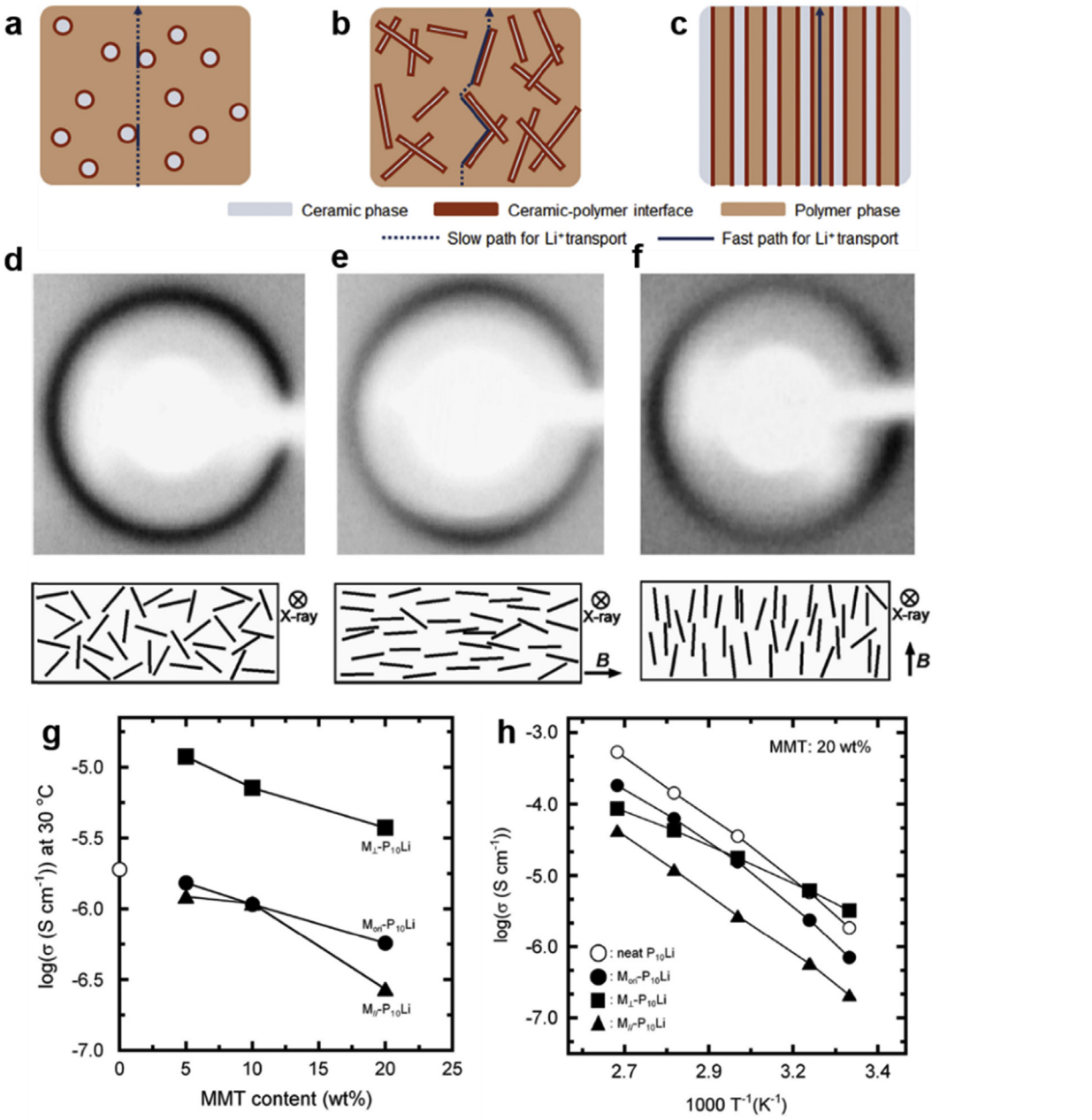

Fig. 5. Evolution of different filler additives in CSSEs. (a) 0D nanoparticles, (b) 1D nanowires, (c) continuous aligned interfaces. Reproduced with permission from American Chemical Society. 2D WAX patterns and schematics of (d) random, (e) horizontally aligned, and (f) vertically aligned MMT layers in PEO/LiClO4 system. (g) Ionic conductivity vs. MMT content and (h) ionic conductivity vs. temperature at different MMT orientations in the CSSE system. Reproduced with permission from Nature publishing groups. CSSE, composite solid-state electrolyte; MMT, montmorillonite; PEO, poly(ethylene oxide).

for lithium batteries [12]. However, the formation of lithium dendrites may short the battery and cause catastrophic safety incidents. Among the various approaches to solving this problem, the development of a solid electrolyte with high physical stability has attracted significant attention [98]. It is well accepted that a thin film of high shear modulus will suppress the formation of Li dendrites [99]. Theoretical calculations have predicted that an electrolyte with a shear modulus of 7 GPa or greater can suppress lithium dendrites because of the compressive force generated by solid polymer electrolyte upon deformation [100]. Therefore, designing solid electrolytes that have strong mechanical properties is important to allow the further application of lithium metal in lithium batteries. With the incorporation of inorganic fillers, composite polymer electrolytes may finally be able to provide satisfactory mechanical properties for the lithium metal anode.

Early results have shown that inert nanoparticle fillers can improve the mechanical properties of composite polymer electrolytes. Weston and Steele [62] first reported that adding 10% α-alumina improved the mechanical properties of the $LiClO_4$/PEO composite polymer electrolyte, especially at an elevated temperature. Compared to the pure $LiClO_4$/PEO polymer electrolyte that would soften and creep at an elevated temperature, the addition of inert filler improved the tolerance of the composite electrolyte to mechanical stress at high temperature (Fig. 7a) [62,101]. In addition to α-alumina, other nanoparticles (e.g. γ-$LiAlO_2$ [102–104], TiO_2 [104], and fumed silica [105,106]) and nanowire fillers (LLTO [79]

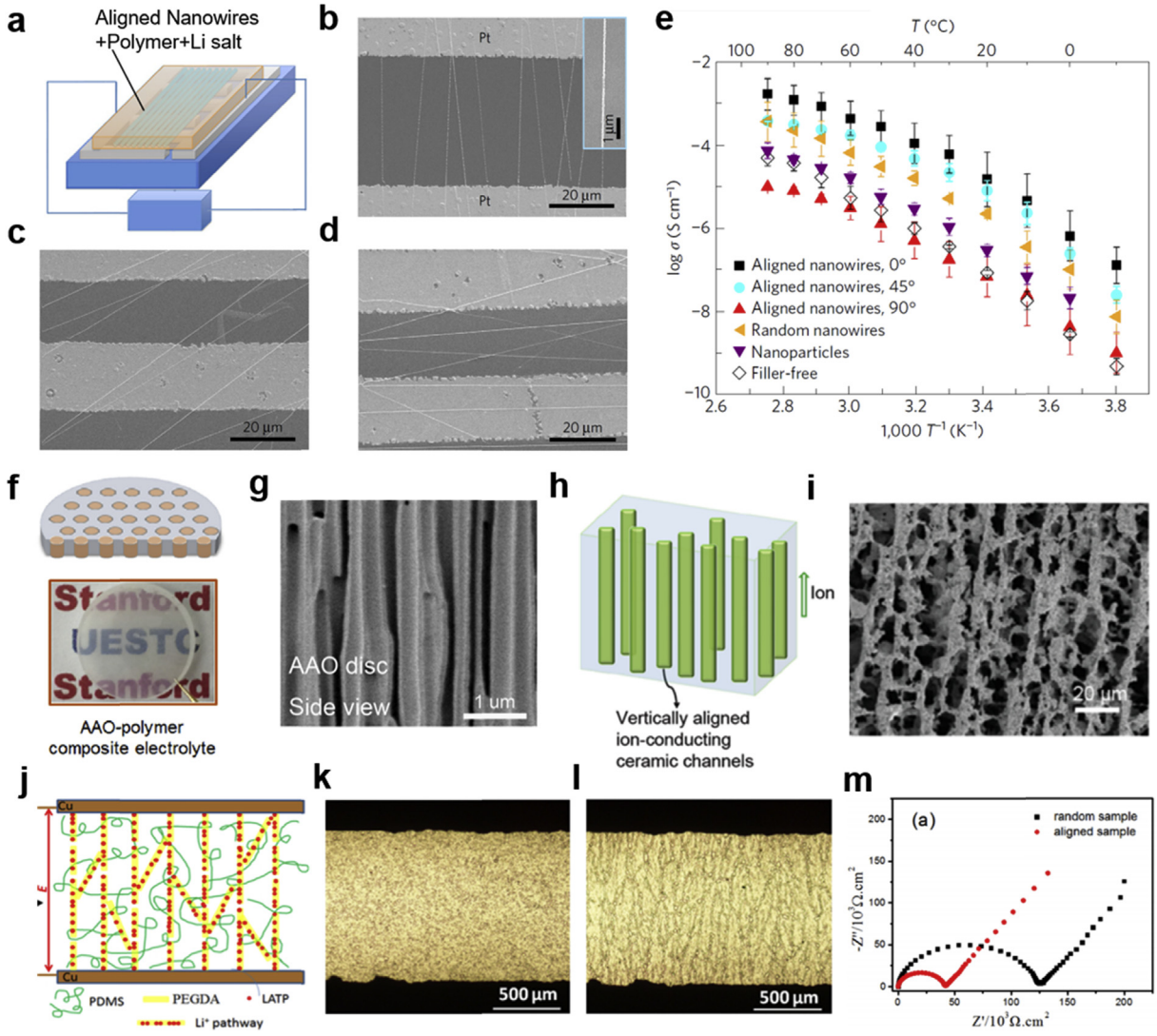

Fig. 6. (a) Schematic image of ionic conductivity measurement in CSSEs with aligned nanowires by interdigitated electrodes. SEM images of nanowires (b) perpendicular to the electrodes, (c) at 45° angle to the electrodes, and (d) parallel to the electrodes. (e) Summary on ionic conductivities of CSSE with aligned nanowires at different angles. Reproduced with permission from Nature publishing groups. (f) Schematic and photo images of PEO-filled AAO CSSE. (g) SEM image of aligned channels in AAO. Reproduced with permission from American Chemical Society. (h–i) Schematic and SEM images of aligned LATP network for CSSEs. Reproduced with permission from American Chemical Society. (j) Schematic of electric field–aligned LATP nanoparticle for CSSE. Photo images of (k) random and (l) aligned nanoparticles in polymer electrolyte. (m) Electrochemical Impedance Spectroscopy (EIS) of samples in (k) and (l). Reproduced with permission from American Chemical Society. AAO, anodized aluminum oxide; CSSE, composite solid-state electrolyte; LATP, $Li_{1.3}Al_{0.3}Ti_{1.7}(PO_4)_3$; PEO, poly(ethylene oxide); SEM, scanning electron microscopy; PDMS, Polydimethylsiloxane; PEGDA, Poly(ethylene glycol) diacrylate.

and LLZO [81]) are also capable of improving the mechanical properties of the composite polymer electrolyte. Very recently, Zhang et al. [90] have shown that a composite solid polymer electrolyte based on a mechanically rigid AAO backbone could effectively suppress lithium dendrite penetration. The composite solid polymer electrolyte allowed Li/Li symmetric cells to be cycled for more than one hundred cycles without shorting (Fig. 7b). In addition, a cross-linking approach has been successfully demonstrated by Choudhury et al. [107] to achieve a freestanding, mechanically robust, and flexible composite polymer electrolyte. Silica functionalized with hydroxide group–terminated PEO was cross-linked with polypropylene oxide-diisocyanate (Fig. 7c). The storage modulus of the cross-linked polymer is 5 orders of magnitude higher than the non–cross-linked suspension (Fig. 7d), which is very promising for the application of lithium dendrite suppression.

Apart from the benefit of forming a mechanically strong network, the addition of inorganic fillers in composite polymer electrolytes also improves the lithium-ion transference number compared to polymer-only electrolytes. Both theoretical and experimental works have shown that electrolytes with high lithium-ion transference numbers are far more able to prevent lithium dendrite formation [54,108,109]. Calculations have shown that when the lithium-ion transference number approaches unity, the electrodeposition of lithium is more uniform and the formation of lithium dendrites is less likely (Fig. 7e) [54]. Benefitting from the high lithium-ion transference number (0.58) and mechanical strength, Li/CSSE/Li symmetric cells and LFP/Li metal batteries utilizing a CSSE (LLZTO/PEO/LiTFSI) demonstrated excellent cycling life without shorting (Fig. 7f) [73].

In addition to the traditional blending of rigid ceramic additives into polymer electrolytes, engineering the polymer matrix itself can provide another effective approach to achieving highly physically stable SSEs. Lopez et al. [110] reported an elastic CSSE that achieved outstanding mechanical properties without sacrificing Li-

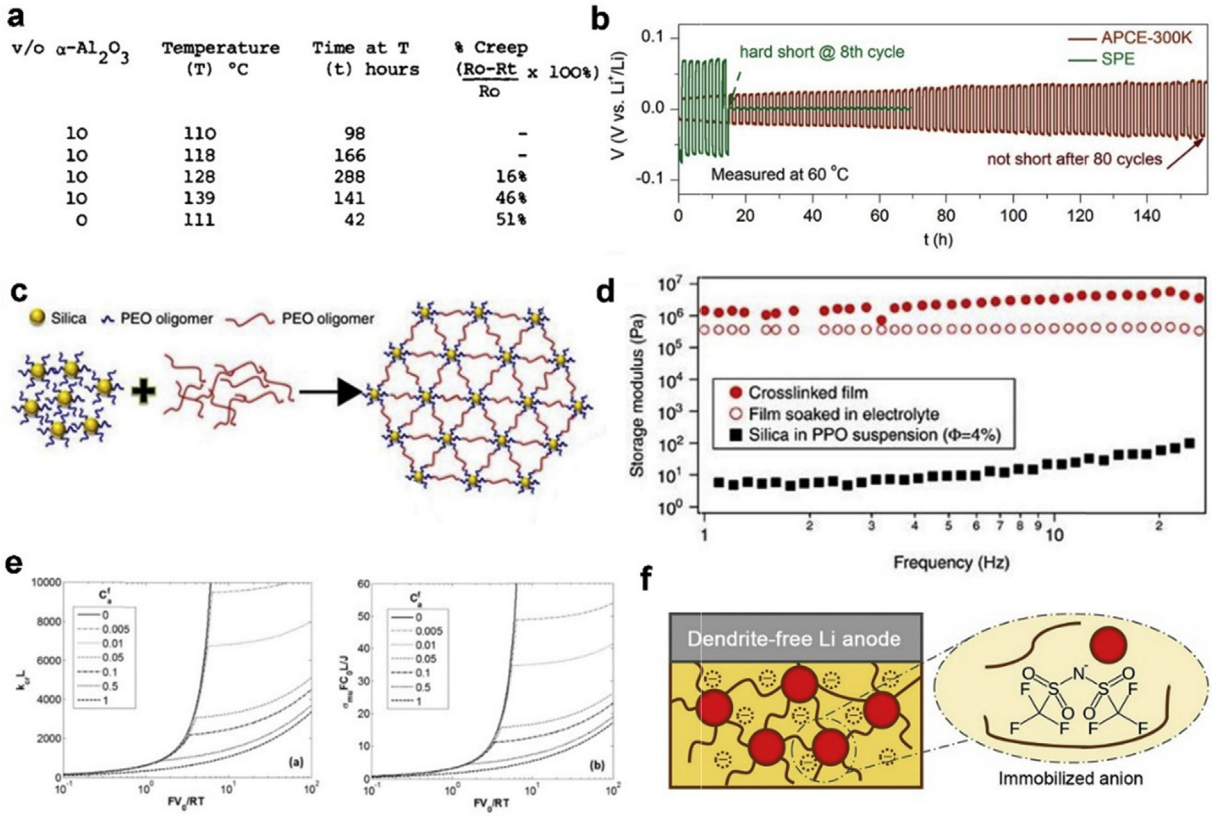

Fig. 7. Physical stability and prevention of lithium dendrite penetration. (a) Mechanical stability of electrolytes above 100 °C. Adapted with permission from Elsevier. (b) Voltage profiles during lithium plating/striping cycling in Li-Li symmetrical cells compared to polymer electrolyte (green) and AAO polymer electrolyte (red) measured at 60 °C with a current density of 0.25 mA/cm^2. Reproduced with permission from the American Chemical Society. (c) Schematic drawing of synthesis route of the free-standing cross-linked nanoparticle-polymer composite. Adapted with permission from Springer. (d) Storage modulus (Pa) as a function of frequency, comparing the dry polymer network and gel electrolyte with a suspension of silica in PPO polymer. Reproduced with permission from Springer. (e) Critical wavenumber and growth rate of most unstable mode at varying overpotentials for various fixed anion fractions. Reproduced with permission from the Electrochemical Society. (f) Schematic drawing of the PEO/LLZTO CSSE for dendrite-free Li metal anode. Reproduced with permission from United States National Academy of Sciences. AAO, anodized aluminum oxide; CSSE, composite solid-state electrolyte; LLZTO, $Li_{6.75}La_3Zr_{1.75}Ta_{0.25}O_{12}$; PEO, poly(ethylene oxide); PPO, poly(propylene oxide).

ion conductivity. As shown in Fig. 8a, the polymer matrix poly(-propylene oxide) (PPO) elastomer (ePPO) was composed of a combination of dynamic hydrogen bonds (to dissipate stress) and static covalent bonds (to provide elasticity). It was then mixed with fumed SiO_2 nanoparticles, LiTFSI salt, and propylene carbonate plasticizer to form the final CSSE. The resulting simultaneously high modulus of resilience (the maximum energy that can be reversibly stored in a material, in this case 0.32 MJ/m^3) and room-temperature ionic conductivity (0.25 mS/cm)—compared to other types of SSEs (Fig. 8b)—demonstrated its great promise in all-solid-state batteries. The superior mechanical properties of this design also ensure the safety of batteries made with ePPO CSSEs. The all-solid-state battery can withstand extreme abuse, such as high load hammer impacts, whereas batteries with the traditional separator/liquid electrolyte setup died easily under the same conditions. This property may be of great significance in a variety of applications such as portable electronics and electrical vehicles.

4. Chemical stability of CSSE

Chemical and electrochemical stabilities represent important parameters for battery electrolytes. For a battery to operate with high stability over long-term cycling, chemical and electrochemical parasitic reactions between the electrolyte and electrode have to be minimized [111–113]. In the ideal case, a stable electrolyte needs to have a highest occupied molecular orbital (HOMO) lower than the electrochemical potential of the cathode and a lowest unoccupied molecular orbital (LUMO) higher than the electrochemical potential of the anode (Fig. 9a). From basic thermodynamics, if the electrochemical potential of the cathode is below the HOMO of the electrolyte, the electrolyte can be oxidized by the cathode. Similarly, if the electrochemical potential of the anode is above the LUMO of the electrolyte, the electrolyte can be reduced by the anode. While kinetic stability can potentially be achieved by forming a solid electrolyte interphase with the addition of electrolyte additives, thermodynamic stability is still highly desired to prevent the electrolyte from being oxidized by the cathode or reduced by the lithium metal anode. The aforementioned parasitic reactions, when accumulated during long-time cycling, may lead to battery failure (high interfacial resistance) and safety hazards (side product accumulation and heat generation).

To improve the electrochemical stability of composite polymer electrolytes, all components (polymer, fillers, and lithium salts) need to be optimized to achieve high overall stability. However, many widely used polymers such as PEO [114,115] can be unstable at high applied potentials and are therefore cannot be used for batteries with high voltage cathodes (Fig. 9b). As PEO represents one of the most conductive and extensively studied polymer electrolyte systems, many approaches have been developed to improve the stability window of PEO-based polymer electrolytes, such as

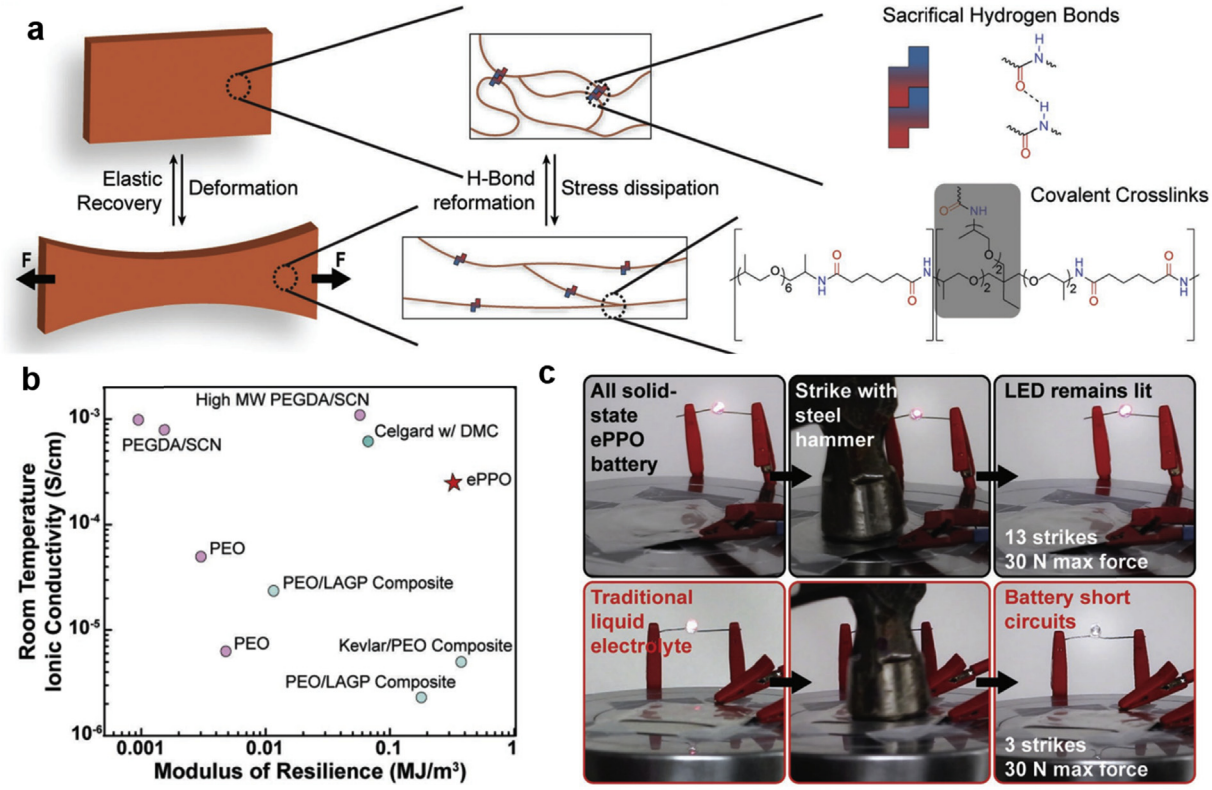

Fig. 8. (a) Schematic and chemical structure of the ePPO CSSE. (b) RT ionic conductivity vs. modulus of resilience of a variety of CSSEs. (c) Digital photographs of ePPO solid-state batteries and traditional liquid electrolyte/Celgard separator batteries undergoing hammer impact tests. Reproduced with permission from John Wiley and Sons. CSSE, composite solid-state electrolyte; ePPO, poly(propylene oxide) elastomer; RT, room temperature; SCN, Succinonitrile; LAGP, $Li_{1+x}Al_xGe_{2-x}(PO_4)3$; DMC, Dimethyl carbonate; LED, Light-emitting diode.

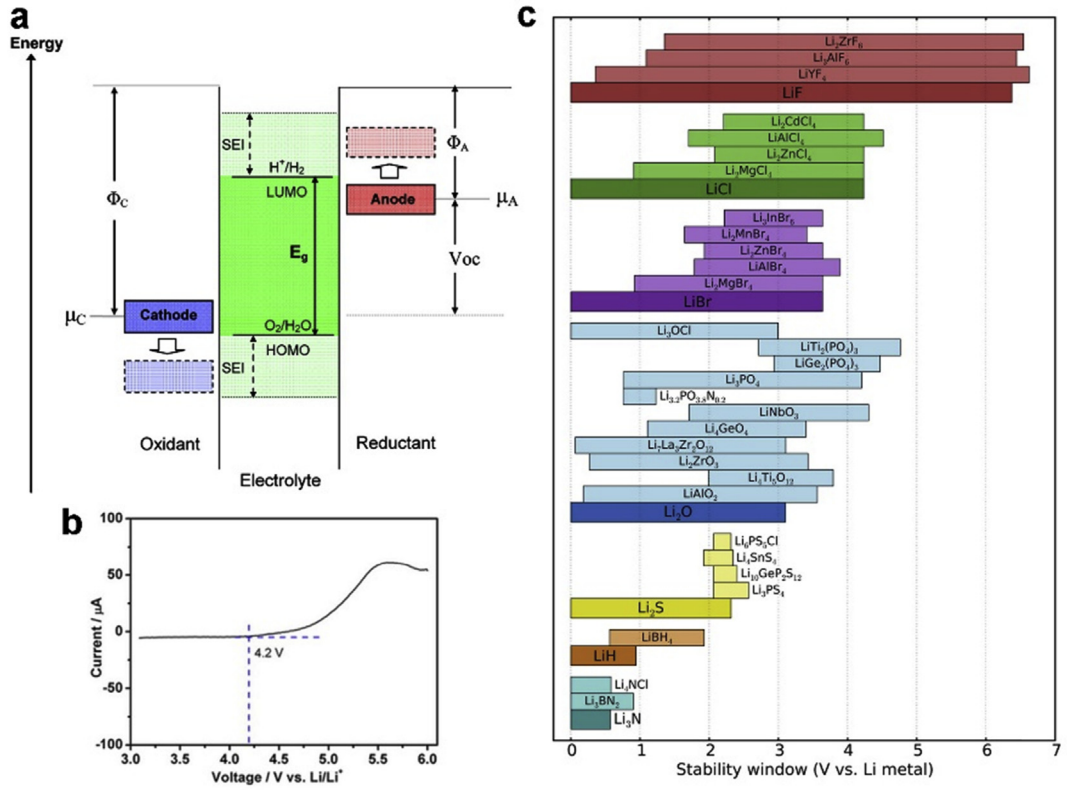

Fig. 9. Electrochemical stability window of PEO and various inorganic fillers. (a) Energy diagram of a battery system. Reproduced with permission from the American Chemical Society. (b) Electrochemical window of PEO electrolyte: linear sweep voltammetry curve of Li/PEO-LiDFOB/stainless steel coin cell at 80 °C. Reproduced with permission from the Electrochemical Society. (c) Electrochemical stability windows of various solid materials. Reproduced with permission from the American Chemical Society. PEO, poly(ethylene oxide); HOMO, highest occupied molecular orbital; LUMO, lowest unoccupied molecular orbital; SEI, solid-electrolyte interface.

developing PEO derivatives with wider electrochemical windows and designing stable interfaces at the PEO/cathode interface [116]. On the other hand, inorganic fillers also experience similar stability issues (Fig. 9c) as many candidates also decompose at the anode and/or cathode side [117–119]. Possible approaches include forming a stable interfacial layer upon electrode/electrolyte contact [120] and replacing non-stable inorganic fillers with stable ones [121]. Even so, the addition of inorganic fillers significantly enhances the interfacial stability of CSSEs against Li metal, compared to pure polymer electrolytes [39].

More importantly, the increasing charging rate and energy density of batteries both pose significant safety concerns and introduce even more requirements for the electrolyte [122]. Although one major goal for solid electrolytes is to increase the safety of batteries by replacing flammable commercial liquid electrolytes, most polymers in solid polymer and composite polymer electrolytes are still flammable. To solve such a challenge, future studies need to focus on the development of non-flammable composite polymer electrolytes while still maintaining their physical and chemical stability.

One direct method to improve the non-flammability of a composite polymer electrolyte is to replace the flammable polymer (such as linear PEO) with a less (or non-)flammable one. A few candidate polymers have been proposed such as polyacrylonitrile [123], fluoropolymers [124], and PEO derivatives (Fig. 10a–b) [57]. Although they all have low flammability, most of these candidate polymers are inferior lithium-ion conductors to PEO. Thus, future research needs to focus on developing non-flammable polymers while still maintaining high lithium-ion conductivity. Another method to improve the non-flammability is to increase the fraction of non-flammable fillers—an approach that has already been demonstrated with liquid electrolytes. For instance, Agrawal et al. has shown that simply increasing the non-flammable content of SiO_2-PEG hairy nanoparticles in flammable carbonate electrolyte can prevent the entire composite electrolyte from igniting [125]. More recently, Liu et al. [126] developed an exciting approach of using thermally triggered flame retardant to suppress fire incidents in batteries. The flame retardant (triphenyl phosphate) was sealed inside a polymer to avoid side reactions with the cathode and anode; when battery temperature is increased, the flame retardant was released to prevent a battery fire (Fig. 10c and d). Although this technique was demonstrated with liquid electrolyte, it can potentially be applied to the CSSE case.

5. Advanced characterization techniques for CSSEs

The design of better CSSEs that possess high ionic conductivity and stable interfaces relies on an in-depth understanding of the relevant electrochemical processes [127,128]. Characterization techniques such as X-ray diffraction (XRD), scanning electron microscopy (SEM), differential scanning calorimetry (DSC), Fourier-transform infrared spectroscopy (FTIR), and Raman spectroscopy are among the most common characterization techniques used to probe the workings of CSSEs. Both XRD and DSC are widely used to characterize the crystallinity of polymers in CSSEs [129]; incidentally, DSC is also capable of providing the glass transition

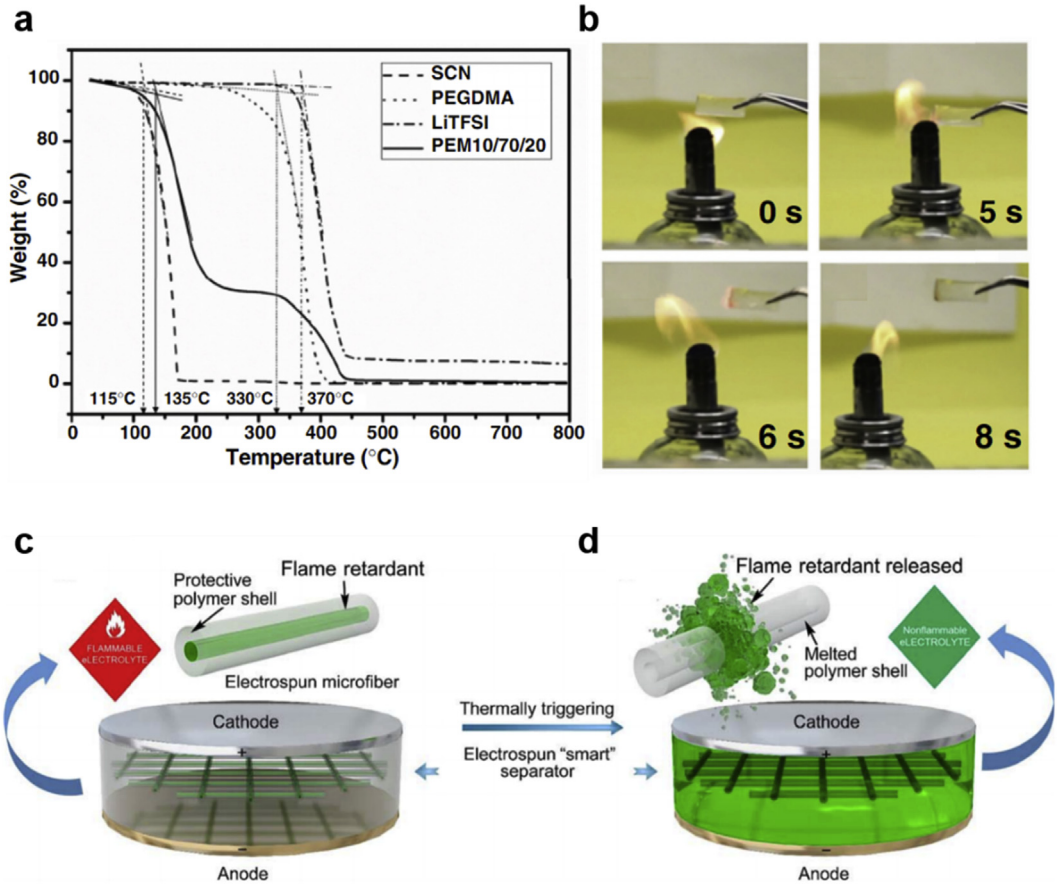

Fig. 10. Materials for lithium-ion battery safety. (a) Thermogravimetric analysis (TGA) thermogram of cross-linked PEO derivative polymer electrolyte and its components. (b) Flame test of PEO derivative polymer electrolyte. Reproduced with permission from Elsevier. (e) Schematic drawing of applying fire retardant to improve battery safety. Reproduced with permission from the American Association for the Advancement of Science. PEO, poly(ethylene oxide); PEGDMA, Polyethylene glycol dimethacrylate.

temperature of the polymer complex in question [130,131]. FTIR and Raman spectroscopy, on the other hand, are often used to determine the polymer's conformational changes, ion dissociation, solvation, etc. [132–135] The mechanical properties such as elastic modulus can be determined with tensile testing or nano-indentation techniques [71,136]. Transmission electron microscopy (TEM) has been widely used to characterize batteries, including SSEs [137–141]. However, it is difficult to obtain useful information for CSSEs with traditional TEM techniques. Despite the power of these different characterization techniques, many important details—such as the mechanism of lithium-ion transport in CSSEs—still remain unelucidated. Again, it is widely proposed that the increased ionic conductivity from the addition of passive fillers is mainly due to the amorphous interfaces between such fillers and their polymer hosts. The ionic transport mechanism of CSSEs with active fillers, however, remains controversial.

As lithium is a light element, it is challenging to probe with regular characterization techniques. As a result, more advanced material characterization methods, such as nuclear magnetic resonance (NMR) spectroscopy, synchrotron X-ray, and neutron scattering techniques, are used to understand the behavior of ASSLBs [142–147]. Zheng et al. [142], for example, used high-resolution solid-state NMR to characterize the Li-ion transport mechanism of CSSEs with LLZO fillers. Fig. 11a shows the schematic of a Li symmetric cell, with both electrodes made from ^{6}Li foil. After cycling, ^{6}Li had entered the LLZO-PEO composite at three different locations, namely the PEO/$LiClO_4$ bulk, the polymer/LLZO interface, and the LLZO particles themselves (Fig. 11b). The ^{6}Li shift obtained from solid-state NMR indicated that the ^{6}Li primarily accumulated in the LLZO particles, which implied that the fastest ionic transport pathway for this particular CSSE was through the active LLZO fillers (Fig. 11c and d). Mackanic et al. also reported using 7Li NMR

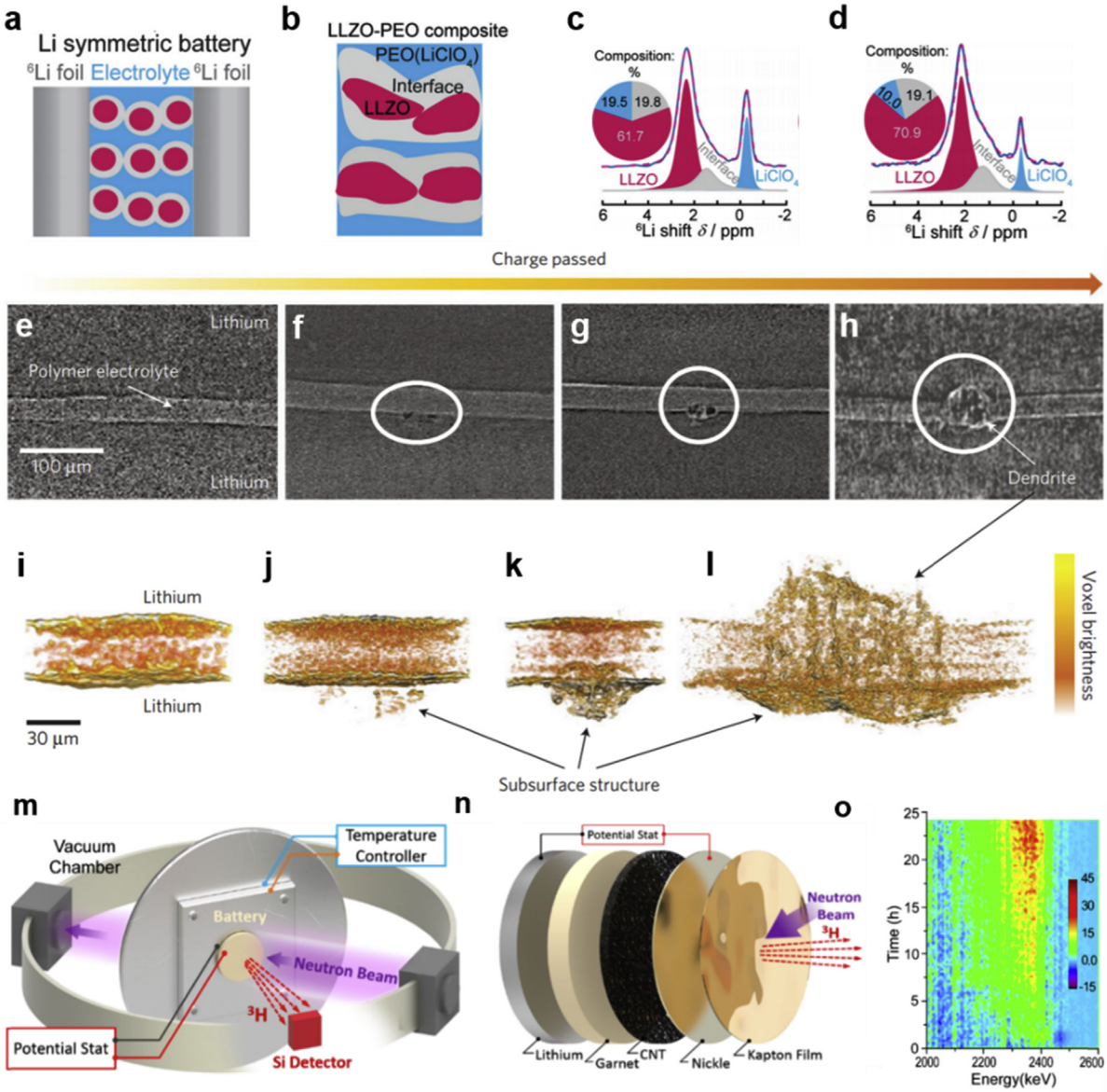

Fig. 11. (a–b) Schematic of LLZO-PEO composite electrolyte with ^{6}Li symmetric battery. (c) ^{6}Li direct polarization and cross-polarization NMR spectra and analysis of LLZO-PEO composite electrolyte. Reproduced with permission from John Wiley and Sons. (e–h) X-Ray tomography images of the evolution of Li dendrites with increasing charge inside symmetric Li-polymer electrolyte-Li structure. Reproduced with permission from Nature publishing group. (i–l) 3D reconstructed volume of cells from (e–h). Schematic of (m) the setup and (n) cell configuration for the *in situ* neutron depth profiling measurement. (o) 2D projection of the neutron depth profiling spectra collected at 5-min intervals during cycling. Reproduced with permission from the American Chemical Society. LLZO, $Li_7La_3Zr_2O_{12}$; NMR, nuclear magnetic resonance; PEO, poly(ethylene oxide).

measurements to detect the loosened O-Li+ coordination in a cross-linked poly(tetrahydrofuran) (xPTHF)/LiTFSI polymer electrolyte system [147]. This structure benefits to a higher Li conductivity and transference number (0.53) compared with a cross-linked PEO system at the same length.

An understanding of Li deposition at the CSSE/anode interface is also crucial for the effective utilization of CSSEs in Li batteries. Although the plating and stripping behavior of Li in liquid electrolyte is well documented, the characterization of Li deposition in CSSEs is rare [148–152]. In one of these few studies, Harry et al. [143] used X-ray tomography to observe Li deposition in the presence of a solid polymer electrolyte. As charge accumulated, the Li proceeded to nucleate, grow, and finally penetrate the solid polymer electrolyte (Fig. 11e–h, Fig. 11i–l). This work suggests that the successful suppression of Li dendrite growth may start with suppressing the nucleation of subsurface structure on the Li metal. Wang et al. [144] reported an *in situ* neutron depth profiling measurement (Fig. 11m and n) of Li deposition in the presence of an LLZO SSE. Owing to the sensitivity of neutrons to light elements such as Li, the authors were able to monitor Li at the electrode/electrolyte interface. This technique could provide not only a method of effectively characterizing the plating/stripping behaviors of ASSLBs but also a way to diagnose short-circuiting within these batteries (Fig. 11o).

6. Processability of CSSEs

The replacement of liquid electrolytes with SSEs represents a major structural/component change in Li batteries. Thus, the processability and compatibility of SSEs with full cells are two of the major concerns for the usability of any type of SSE. Schematic images of a hard, ceramic SSE full cell and a soft/flexible polymer/composite SSE full cell are shown in Fig. 12a and b, respectively. Digital photographs of ceramic-type SSEs such as Li10GeP2S12 (LGPS) (Fig. 12c, c3 displays a pulverized solid electrolyte after cycling in a full cell) [153] and LLZO [27] (Fig. 12e) are also shown as examples. The thick, rigid ceramic films inhibit the flexibility of the full cells, and their brittle nature may add extra concerns to the damper system of some applications (i.e. electrical vehicles) to avoid risks such as short circuiting. The flexible CSSEs, on the other hand, are both easy to fabricate/handle and compatible with state-of-the-art Li-ion battery technologies. The aforementioned ePPO CSSE, in fact, can even withstand abuses such as puncturing and stretching, as shown in Fig. 12d [110]. Pouch-type cells with CSSEs in full-cell configurations have also been reported, as shown in Fig. 12f [73]. Because of their flexibility, the CSSEs in these cells can continue to function properly even when bended or folded [73,110]. Other concerns, such as electrolyte thickness, are nevertheless still issues for both ceramic SSE- and CSSE-based electrolytes. Because

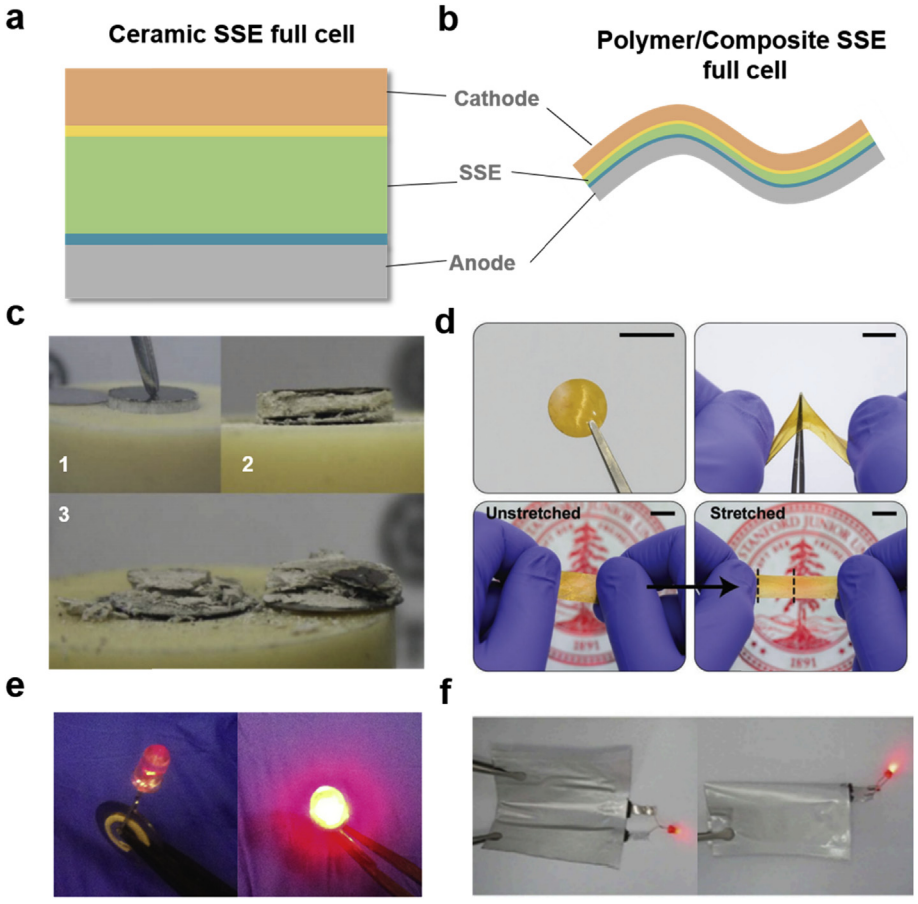

Fig. 12. Full-cell schematics of all-solid-state Li batteries utilizing (a) ceramic solid-state electrolyte and (b) CSSE. Digital photographs of the aftermath of ceramic (c) LGPS electrolyte tests in a full cell and (d) ePPO electrolyte abuse tests. Reproduced with permission from John Wiley and Sons. Digital photographs of (e) LLZO-based and (f) CSSE-based full-cell demonstration. Reproduced with permission from Nature publishing group and National Academy of Sciences, USA. CSSE, composite solid-state electrolyte; ePPO, poly (propylene oxide) elastomer; LLZO, $Li_7La_3Zr_2O_{12}$; SSE, solid-state electrolyte.

both types of SSE weigh significantly more than typical liquid electrolyte/separator systems, it is feared that their implementation may lead to a decrease in energy density [154].

7. Outlook

After the ceaseless efforts of researchers over the past few decades, CSSEs now obtain high room-temperature ionic conductivity (10^{-4} S/cm), high mechanical stability, high chemical stability, and excellent processability, all of which show great promise for ASSLBs. Still, the lack of large-scale, commercialized ASSLB production, despite the widespread demand for safe, high energy density batteries, is indicative of the challenges inhibiting their implementation. Future directions for improving CSSEs include, but are not limited to (1) Obtaining higher ionic conductivity and cation transference number. Although an ionic conductivity of 10^{-4} S/cm can be realized with CSSEs, it is still lower than that of some ceramic SSEs and liquid electrolytes. Owing to their lower ionic conductivity, batteries based on CSSEs are reported to cycle best at elevated temperatures and generally cycle poorly at room temperature. (2) Achieving a higher electrochemical stability window for CSSEs. To date, most CSSEs are based on PEO, which is known to decompose at > 4.0 V (vs. Li/Li^+). Modifications to PEO or the creation of entirely new polymers are needed to pair these electrolytes with high-voltage cathodes such as Lithium Nickel Manganese Cobalt Oxide (NMC) materials and thus achieve high energy density batteries. (3) Improving interface stability. The absence of a lower, more stable interface resistance at the Li metal side is also a major obstacle for faster cycling at ambient temperature. (4) Designing thinner and lower density CSSEs that still retain satisfactory mechanical properties. The thickness of CSSEs and other SSEs in existing literature generally exceeds 100 μm, making these solid electrolytes much thicker and heavier than their liquid electrolyte/separator counterparts. This thickness could potentially compromise the energy density of ASSLBs, although the tight packing of ASSLBs is still an advantage over liquid electrolyte–based batteries, and could partially mitigate this drawback. (5) Developing more advanced characterization techniques and simulations. These methods would make great progress toward elucidating phenomena such as ion transport mechanisms and electrolyte/electrode interfacial properties. With this crucial information, the development of CSSEs for ASSLBs could improve tremendously in the years to come.

Acknowledgment

The work was supported by the Assistant Secretary for Energy Efficiency and Renewable Energy, Office of Vehicle Technologies of the US Department of Energy, under the Battery Materials Research (BMR) program and Battery 500 Consortium program. The authors would also like to thank the discussions and valuable suggestions from Dr. Feifei Shi and Dr. Kai Liu.

Appendix A. Supplementary data

Supplementary data to this article can be found online at https://doi.org/10.1016/j.mtnano.2018.12.003.

References

[1] M. Armand, J.M. Tarascon, Building better batteries, Nature 451 (2008) 652–657, https://doi.org/10.1038/451652a.
[2] J.M. Tarascon, M. Armand, Issues and challenges facing rechargeable lithium batteries, Nature 414 (2001) 359–367, https://doi.org/10.1038/35104644.
[3] P.G. Bruce, S.A. Freunberger, L.J. Hardwick, J.-M. Tarascon, Li–O2 and Li–S batteries with high energy storage, Nat. Mater. 11 (2012) 19–29, https://doi.org/10.1038/nmat3237.
[4] Y. Sun, N. Liu, Y. Cui, Promises and challenges of nanomaterials for lithium-based rechargeable batteries, Nat. Energy 1 (2016), https://doi.org/10.1038/nenergy.2016.71.
[5] J. Lu, Z. Chen, Z. Ma, F. Pan, L.A. Curtiss, K. Amine, The role of nanotechnology in the development of battery materials for electric vehicles, Nat. Nanotechnol. 11 (2016) 1031–1038, https://doi.org/10.1038/nnano.2016.207.
[6] K. Xu, Nonaqueous liquid electrolytes for lithium-based rechargeable batteries, Chem. Rev. 104 (2004) 4303–4417, https://doi.org/10.1021/cr030203g.
[7] K. Xu, Electrolytes and interphases in Li-ion batteries and beyond, Chem. Rev. 114 (2014) 11503–11618, https://doi.org/10.1021/cr500003w.
[8] W. Bao, J. Wan, X. Han, X. Cai, H. Zhu, D. Kim, D. Ma, Y. Xu, J.N. Munday, H.D. Drew, M.S. Fuhrer, L. Hu, Approaching the limits of transparency and conductivity in graphitic materials through lithium intercalation, Nat. Commun. 5 (2014), https://doi.org/10.1038/ncomms5224.
[9] S. Chu, Y. Cui, N. Liu, The path towards sustainable energy, Nat. Mater. 16 (2016) 16–22, https://doi.org/10.1038/nmat4834.
[10] Q. Pang, X. Liang, C.Y. Kwok, L.F. Nazar, Advances in lithium-sulfur batteries based on multifunctional cathodes and electrolytes, Nat. Energy 1 (2016), https://doi.org/10.1038/nenergy.2016.132.
[11] J. Wan, A.F. Kaplan, J. Zheng, X. Han, Y. Chen, N.J. Weadock, N. Faenza, S. Lacey, T. Li, J. Guo, L. Hu, Two dimensional silicon nanowalls for lithium ion batteries, J. Mater. Chem. 2 (2014), https://doi.org/10.1039/c3ta13546b.
[12] D. Lin, Y. Liu, Y. Cui, Reviving the lithium metal anode for high-energy batteries, Nat. Nanotechnol. 12 (2017) 194–206, https://doi.org/10.1038/nnano.2017.16.
[13] Y. Liu, G. Zhou, K. Liu, Y. Cui, Design of Complex Nanomaterials for Energy Storage: Past Success and Future Opportunity, Acc. Chem. Res. 50 (2017) 2895–2905, https://doi.org/10.1021/acs.accounts.7b00450.
[14] J. Xie, J. Wang, H.R. Lee, K. Yan, Y. Li, F. Shi, W. Huang, A. Pei, G. Chen, R. Subbaraman, J. Christensen, Y. Cui, Engineering stable interfaces for three-dimensional lithium metal anodes, Sci. Adv. 4 (2018), https://doi.org/10.1126/sciadv.aat5168 eaat5168.
[15] J. Lu, Y.J. Lee, X. Luo, K.C. Lau, M. Asadi, H.H. Wang, S. Brombosz, J. Wen, D. Zhai, Z. Chen, D.J. Miller, Y.S. Jeong, J.B. Park, Z.Z. Fang, B. Kumar, A. Salehi-Khojin, Y.K. Sun, L.A. Curtiss, K. Amine, A lithium-oxygen battery based on lithium superoxide, Nature 529 (2016) 377–382, https://doi.org/10.1038/nature16484.
[16] J. Lu, L. Li, J.B. Park, Y.K. Sun, F. Wu, K. Amine, Aprotic and aqueous Li-O2 batteries, Chem. Rev. 114 (2014) 5611–5640, https://doi.org/10.1021/cr400573b.
[17] X. Ji, K.T. Lee, L.F. Nazar, A highly ordered nanostructured carbon-sulphur cathode for lithium-sulphur batteries, Nat. Mater. 8 (2009) 500–506, https://doi.org/10.1038/nmat2460.
[18] Y. Liang, Y. Yao, Positioning organic electrode materials in the battery landscape, Joule (2018), https://doi.org/10.1016/j.joule.2018.07.008.
[19] T.F. Miller, Z.G. Wang, G.W. Coates, N.P. Balsara, Designing polymer electrolytes for safe and high capacity rechargeable lithium batteries, Acc. Chem. Res. 50 (2017) 590–593, https://doi.org/10.1021/acs.accounts.6b00568.
[20] G. Zheng, S.W. Lee, Z. Liang, H.W. Lee, K. Yan, H. Yao, H. Wang, W. Li, S. Chu, Y. Cui, Interconnected hollow carbon nanospheres for stable lithium metal anodes, Nat. Nanotechnol. 9 (2014) 618–623, https://doi.org/10.1038/nnano.2014.152.
[21] D. Lin, Y. Liu, Z. Liang, H.W. Lee, J. Sun, H. Wang, K. Yan, J. Xie, Y. Cui, Layered reduced graphene oxide with nanoscale interlayer gaps as a stable host for lithium metal anodes, Nat. Nanotechnol. 11 (2016) 626–632, https://doi.org/10.1038/nnano.2016.32.
[22] Y. Lu, Z. Tu, L.A. Archer, Stable lithium electrodeposition in liquid and nanoporous solid electrolytes, Nat. Mater. 13 (2014) 961. https://doi.org/10.1038/nmat4041.
[23] Y. Liu, D. Lin, Y. Jin, K. Liu, X. Tao, Q. Zhang, X. Zhang, Y. Cui, Transforming from planar to three-dimensional lithium with flowable interphase for solid lithium metal batteries, Sci. Adv. 3 (2017) 1–11, https://doi.org/10.1126/sciadv.aao0713.
[24] C.P. Yang, Y.X. Yin, S.F. Zhang, N.W. Li, Y.G. Guo, Accommodating lithium into 3D current collectors with a submicron skeleton towards long-life lithium metal anodes, Nat. Commun. 6 (2015), https://doi.org/10.1038/ncomms9058.
[25] J. Xie, L. Liao, Y. Gong, Y. Li, F. Shi, A. Pei, J. Sun, R. Zhang, B. Kong, R. Subbaraman, J. Christensen, Y. Cui, Stitching h-BN by atomic layer deposition of LiF as a stable interface for lithium metal anode, Sci. Adv. 3 (2017), https://doi.org/10.1126/sciadv.aao3170.
[26] K. Liu, A. Pei, H.R. Lee, B. Kong, N. Liu, D. Lin, Y. Liu, C. Liu, P. chun Hsu, Z. Bao, Y. Cui, Lithium metal anodes with an adaptive "Solid-Liquid" interfacial protective layer, J. Am. Chem. Soc. 139 (2017) 4815–4820, https://doi.org/10.1021/jacs.6b13314.
[27] X. Han, Y. Gong, K. Fu, X. He, G.T. Hitz, J. Dai, A. Pearse, B. Liu, H. Wang, G. Rubloff, Y. Mo, V. Thangadurai, E.D. Wachsman, L. Hu, Negating interfacial impedance in garnet-based solid-state Li metal batteries, Nat. Mater. 16 (2017) 572–579, https://doi.org/10.1038/nmat4821.
[28] J.C. Bachman, S. Muy, A. Grimaud, H.H. Chang, N. Pour, S.F. Lux, O. Paschos, F. Maglia, S. Lupart, P. Lamp, L. Giordano, Y. Shao-Horn, Inorganic solid-state

electrolytes for lithium batteries: mechanisms and properties governing ion conduction, Chem. Rev. 116 (2016) 140–162, https://doi.org/10.1021/acs.chemrev.5b00563.
[29] A. Manthiram, X. Yu, S. Wang, Lithium battery chemistries enabled by solid-state electrolytes, Nat. Rev. Mater. 2 (2017), https://doi.org/10.1038/natrevmats.2016.103.
[30] X. Yao, D. Liu, C. Wang, P. Long, G. Peng, Y.-S. Hu, H. Li, L. Chen, X. Xu, High-energy all-solid-state lithium batteries with ultralong cycle life, Nano Lett. 16 (2016) 7148–7154, https://doi.org/10.1021/acs.nanolett.6b03448.
[31] Y. Jin, K. Liu, J. Lang, D. Zhuo, Z. Huang, C. an Wang, H. Wu, Y. Cui, An intermediate temperature garnet-type solid electrolyte-based molten lithium battery for grid energy storage, Nat. Energy (2018) 1–7, https://doi.org/10.1038/s41560-018-0198-9.
[32] Y. Gao, D. Wang, Y. Li, Z. Yu, T. Mallouk, D. Wang, Salt-based organic-inorganic nanocomposites: towards a stable lithium metal/$Li_{10}GeP_2S_{12}$ solid electrolyte interface, Angew. Chem. Int. Ed. 0 (2018), https://doi.org/10.1002/anie.201807304.
[33] J. Lau, R.H. DeBlock, D.M. Butts, D.S. Ashby, C.S. Choi, B.S. Dunn, Sulfide solid electrolytes for lithium battery applications, Adv. Energy Mater. (2018) 1800933, https://doi.org/10.1002/aenm.201800933.
[34] Y. Shen, Y. Zhang, S. Han, J. Wang, Z. Peng, L. Chen, Unlocking the energy capabilities of lithium metal electrode with solid-state electrolytes, Joule (2018), https://doi.org/10.1016/j.joule.2018.06.021.
[35] J. Dai, C. Yang, C. Wang, G. Pastel, L. Hu, Interface engineering for garnet-based solid-state lithium-metal batteries: materials, structures, and characterization, Adv. Mater. 0 (2018) 1802068, https://doi.org/10.1002/adma.201802068.
[36] A. Manuel Stephan, K.S. Nahm, Review on composite polymer electrolytes for lithium batteries, Polymer 47 (2006) 5952–5964, https://doi.org/10.1016/j.polymer.2006.05.069.
[37] N.B. Aetukuri, S. Kitajima, E. Jung, L.E. Thompson, K. Virwani, M.L. Reich, M. Kunze, M. Schneider, W. Schmidbauer, W.W. Wilcke, D.S. Bethune, J.C. Scott, R.D. Miller, H.C. Kim, Flexible ion-conducting composite membranes for lithium batteries, Adv. Energy Mater. 5 (2015), https://doi.org/10.1002/aenm.201500265.
[38] Y. Ren, Y. Shen, Y. Lin, C.W. Nan, Direct observation of lithium dendrites inside garnet-type lithium-ion solid electrolyte, Electrochem. Commun. 57 (2015) 27–30, https://doi.org/10.1016/j.elecom.2015.05.001.
[39] B. Kumar, L.G. Scanlon, Polymer-ceramic composite electrolytes, J. Power Sources 52 (1994) 261–268, https://doi.org/10.1016/0378-7753(94)02147-3.
[40] D.E. Fenton, J.M. Parker, P.V. Wright, Complexes of alkali metal ions with poly(ethylene oxide), Polymer 14 (1973) 589, https://doi.org/10.1016/0032-3861(73)90146-8.
[41] P.V. Wright, Electrical conductivity in ionic complexes of poly(ethylene oxide), Br. Polym. J. 7 (1975) 319–327, https://doi.org/10.1002/pi.4980070505.
[42] M. Armand, M.B. Chabagno, J.M. Duclot, Poly-ethers as solid electrolytes, in: P. Vashitshta, J.N. Mundy, G.K. Shenoy (Eds.), Fast Ion Transport in Solids. Electrodes and Electrolyte, North Holland Publishers, 1979.
[43] M. Armand, Polymer solid electrolytes - an overview, Solid State Ionics 9 (10) (1983) 745–754, https://doi.org/10.1016/0167-2738(83)90083-8.
[44] Z. Wang, B. Huang, H. Huang, L. Chen, R. Xue, F. Wang, Investigation of the position of Li^+ions in a polyacrylonitrile-based electrolyte by Raman and infrared spectroscopy, Electrochim. Acta 41 (1996), https://doi.org/10.1016/0013-4686(95)00392-4.
[45] H. Hong, C. Liquan, H. Xuejie, X. Rongjian, Studies on PAN-based lithium salt complex, Electrochim. Acta 37 (1992) 1671–1673, https://doi.org/10.1016/0013-4686(92)80135-9.
[46] Y.F. Zhou, S. Xie, X.W. Ge, C.H. Chen, K. Amine, Preparation of rechargeable lithium batteries with poly(methyl methacrylate) based gel polymer electrolyte by in situ γ-ray irradiation-induced polymerization, J. Appl. Electrochem. 34 (2004) 1119–1125, https://doi.org/10.1007/s10800-004-2726-5.
[47] G.B. Appetecchi, F. Croce, B. Scrosati, Kinetics and stability of the lithium electrode in poly(methylmethacrylate)-based gel electrolytes, Electrochim. Acta 40 (1995) 991–997, https://doi.org/10.1016/0013-4686(94)00345-2.
[48] M. Alamgir, K.M. Abraham, Li ion conductive electrolytes based on poly(vinyl chloride), J. Electrochem. Soc. 140 (1993) L96–L97, https://doi.org/10.1149/1.2221654.
[49] Y. Tominaga, K. Yamazaki, Fast Li-ion conduction in poly(ethylene carbonate)-based electrolytes and composites filled with TiO2nanoparticles, Chem. Commun. 50 (2014) 4448–4450, https://doi.org/10.1039/c3cc49588d.
[50] H.S. Choe, J. Giaccai, M. Alamgir, K.M. Abraham, Preparation and characterization of poly(vinyl-sulfone)-based and poly(vinylidene-fluoride)-based electrolytes, Electrochim. Acta 40 (1995) 2289–2293, https://doi.org/10.1016/0013-4686(95)00180-m.
[51] Z. Gadjourova, Y.G. Andreev, D.P. Tunstall, P.G. Bruce, Ionic conductivity in crystalline polymer electrolytes, Nature 412 (2001) 520–523, https://doi.org/10.1038/35087538.
[52] A.M. Christie, S.J. Lilley, E. Staunton, Y.G. Andreev, P.G. Bruce, Increasing the conductivity of crystalline polymer electrolytes, Nature 433 (2005) 50–53, https://doi.org/10.1038/nature03186.
[53] Z. Xue, D. He, X. Xie, Poly(ethylene oxide)-based electrolytes for lithium-ion batteries, J. Mater. Chem. A. 3 (2015) 19218–19253, https://doi.org/10.1039/C5TA03471J.
[54] M.D. Tikekar, L.A. Archer, D.L. Koch, Stability analysis of electrodeposition across a structured electrolyte with immobilized anions, J. Electrochem. Soc. 161 (2014) A847–A855, https://doi.org/10.1149/2.085405jes.
[55] W.S. Young, W.F. Kuan, T.H. Epps, Block copolymer electrolytes for rechargeable lithium batteries, J. Polym. Sci. B Polym. Phys. 52 (2014) 1–16, https://doi.org/10.1002/polb.23404.
[56] C. Wang, T. Sakai, O. Watanabe, K. Hirahara, T. Nakanishi, All solid-state lithium-polymer battery using a self-cross-linking polymer electrolyte, J. Electrochem. Soc. 150 (2003) A1166, https://doi.org/10.1149/1.1593652.
[57] J. Cao, R. He, T. Kyu, Fire retardant, superionic solid state polymer electrolyte membranes for lithium ion batteries, Curr. Opin. Chem. Eng. 15 (2017) 68–75, https://doi.org/10.1016/j.coche.2016.12.001.
[58] J. Zhang, L. Yue, P. Hu, Z. Liu, B. Qin, B. Zhang, Q. Wang, G. Ding, C. Zhang, X. Zhou, J. Yao, G. Cui, L. Chen, Taichi-inspired rigid-flexible coupling cellulose-supported solid polymer electrolyte for high-performance lithium batteries, Sci. Rep. 4 (2014), https://doi.org/10.1038/srep06272.
[59] B. Wu, L. Wang, Z. Li, M. Zhao, K. Chen, S. Liu, Y. Pu, J. Li, Performance of "Polymer-in-Salt" electrolyte PAN-LiTFSI enhanced by graphene oxide filler, J. Electrochem. Soc. 163 (2016) A2248–A2252, https://doi.org/10.1149/2.0531610jes.
[60] C. Tang, K. Hackenberg, Q. Fu, P.M. Ajayan, H. Ardebili, High ion conducting polymer nanocomposite electrolytes using hybrid nanofillers, Nano Lett. 12 (2012) 1152–1156, https://doi.org/10.1021/nl202692y.
[61] C. Gerbaldi, J.R. Nair, M.A. Kulandainathan, R.S. Kumar, C. Ferrara, P. Mustarelli, A.M. Stephan, Innovative high performing metal organic framework (MOF)-laden nanocomposite polymer electrolytes for all-solid-state lithium batteries, J. Mater. Chem. A. 2 (2014) 9948–9954, https://doi.org/10.1039/C4TA01856G.
[62] J.E. Weston, B.C.H. Steele, Effects of inert fillers on the mechanical and electrochemical properties of lithium salt-poly(ethylene oxide) polymer electrolytes, Solid State Ionics 7 (1982) 75–79, https://doi.org/10.1016/0167-2738(82)90072-8.
[63] M.A.K.L. Dissanayake, P.A.R.D. Jayathilaka, R.S.P. Bokalawala, I. Albinsson, B.E. Mellander, Effect of concentration and grain size of alumina filler on the ionic conductivity enhancement of the (PEO)9LiCF3SO3:Al2O3 composite polymer electrolyte, J. Power Sources (2003) 409–414, https://doi.org/10.1016/S0378-7753(03)00262-3.
[64] J. Płocharski, W. Wieczorek, J. Przyłuski, K. Such, Mixed solid electrolytes based on poly(ethylene oxide), Appl. Phys. A 49 (1989) 55–60, https://doi.org/10.1007/BF00615464.
[65] F. Croce, G.B. Appetecchi, L. Persi, B. Scrosati, Nanocomposite polymer electrolytes for lithium batteries, Nature 394 (1998) 456–458, https://doi.org/10.1038/28818.
[66] F. Croce, L.L. Persi, B. Scrosati, F. Serraino-Fiory, E. Plichta, M.A. Hendrickson, Role of the ceramic fillers in enhancing the transport properties of composite polymer electrolytes, Electrochim. Acta 46 (2001) 2457–2461, https://doi.org/10.1016/S0013-4686(01)00458-3.
[67] W. Wieczorek, A. Zalewska, D. Raducha, Z. Florjańczyk, J.R. Stevens, Composite polyether electrolytes with lewis acid type additives, J. Phys. Chem. B 102 (1998) 352–360, https://doi.org/10.1021/jp972727o.
[68] H.-M. Xiong, Z.-D. Wang, D.-P. Xie, L. Cheng, Y.-Y. Xia, Stable polymer electrolytes based on polyether-grafted ZnO nanoparticles for all-solid-state lithium batteries, J. Mater. Chem. 16 (2006) 1345–1346.
[69] D. Lin, W. Liu, Y. Liu, H.R. Lee, P.C. Hsu, K. Liu, Y. Cui, High ionic conductivity of composite solid polymer electrolyte via in situ synthesis of monodispersed SiO2 nanospheres in poly(ethylene oxide), Nano Lett. 16 (2016) 459–465, https://doi.org/10.1021/acs.nanolett.5b04117.
[70] W. Liu, D. Lin, J. Sun, G. Zhou, Y. Cui, Improved lithium ionic conductivity in composite polymer electrolytes with oxide-ion conducting nanowires, ACS Nano 10 (2016) 11407–11413, https://doi.org/10.1021/acsnano.6b06797.
[71] D. Lin, P.Y. Yuen, Y. Liu, W. Liu, N. Liu, R.H. Dauskardt, Y. Cui, A silica-aerogel-reinforced composite polymer electrolyte with high ionic conductivity and high modulus, Adv. Mater. (2018) 1802661, https://doi.org/10.1002/adma.201802661.
[72] S. Skaarup, K. West, B. Zachau-Christiansen, Mixed phase solid electrolytes, Solid State Ionics 28 (30) (1988) 975–978, https://doi.org/10.1016/0167-2738(88)90314-1.
[73] C.-Z. Zhao, X.-Q. Zhang, X.-B. Cheng, R. Zhang, R. Xu, P.-Y. Chen, H.-J. Peng, J.-Q. Huang, Q. Zhang, An anion-immobilized composite electrolyte for dendrite-free lithium metal anodes, Proc. Natl. Acad. Sci. Unit. States Am. (2017) 201708489, https://doi.org/10.1073/pnas.1708489114.
[74] L. Chen, Y. Li, S.-P. Li, L.-Z. Fan, C.-W. Nan, J.B. Goodenough, PEO/garnet composite electrolytes for solid-state lithium batteries: From "ceramic-in-polymer" to "polymer-in-ceramic, Nanomater. Energy 46 (2018) 176–184. https://doi.org/10.1016/j.nanoen.2017.12.037.
[75] A.S. Pandian, X.C. Chen, J. Chen, B.S. Lokitz, R.E. Ruther, G. Yang, K. Lou, J. Nanda, F.M. Delnick, N.J. Dudney, Facile and scalable fabrication of polymer-ceramic composite electrolyte with high ceramic loadings, J. Power Sources 390 (2018) 153–164, https://doi.org/10.1016/j.jpowsour.2018.04.006.
[76] W. Wang, E. Yi, A.J. Fici, R.M. Laine, J. Kieffer, Lithium ion conducting poly(ethylene oxide)-based solid electrolytes containing active or passive ceramic nanoparticles, J. Phys. Chem. C 121 (2017) 2563–2573, https://doi.org/10.1021/acs.jpcc.6b11136.

[77] Y. Zhao, C. Wu, G. Peng, X. Chen, X. Yao, Y. Bai, F. Wu, S. Chen, X. Xu, A new solid polymer electrolyte incorporating Li10GeP2S12 into a polyethylene oxide matrix for all-solid-state lithium batteries, J. Power Sources 301 (2016) 47–53. https://doi.org/10.1016/j.jpowsour.2015.09.111.

[78] C. Wang, X.-W. Zhang, A.J. Appleby, Solvent-free composite PEO-ceramic fiber/mat electrolytes for lithium secondary cells, J. Electrochem. Soc. 152 (2005) A205, https://doi.org/10.1149/1.1828952.

[79] W. Liu, N. Liu, J. Sun, P.C. Hsu, Y. Li, H.W. Lee, Y. Cui, Ionic conductivity enhancement of polymer electrolytes with ceramic nanowire fillers, Nano Lett. 15 (2015) 2740–2745, https://doi.org/10.1021/acs.nanolett.5b00600.

[80] T. Yang, J. Zheng, Q. Cheng, Y.Y. Hu, C.K. Chan, Composite polymer electrolytes with Li7La3Zr2O12Garnet-type nanowires as ceramic fillers: mechanism of conductivity enhancement and role of doping and morphology, ACS Appl. Mater. Interfaces 9 (2017) 21773–21780, https://doi.org/10.1021/acsami.7b03806.

[81] K. Kelvin Fu, Y. Gong, J. Dai, A. Gong, X. Han, Y. Yao, C. Wang, Y. Wang, Y. Chen, C. Yan, Y. Li, E.D. Wachsman, L. Hu, Flexible, solid-state, ion-conducting membrane with 3D garnet nanofiber networks for lithium batteries, Proc. Natl. Acad. Sci. Unit. States Am. 113 (2016) 7094–7099, https://doi.org/10.1073/pnas.1600422113.

[82] Y. Gong, K. Fu, S. Xu, J. Dai, T.R. Hamann, L. Zhang, G.T. Hitz, Z. Fu, Z. Ma, D.W. McOwen, X. Han, L. Hu, E.D. Wachsman, Lithium-ion conductive ceramic textile: A new architecture for flexible solid-state lithium metal batteries, Mater. Today (2018), https://doi.org/10.1016/j.mattod.2018.01.001.

[83] D. Golodnitsky, E. Livshits, R. Kovarsky, E. Peled, S.H. Chung, S. Suarez, S.G. Greenbaum, New generation of ordered polymer electrolytes for lithium batteries, Electrochem. Solid State Lett. 7 (2004) A412, https://doi.org/10.1149/1.1803434.

[84] D. Golodnitsky, E. Strauss, E. Peled, S. Greenbaum, Review—on order and disorder in polymer electrolytes, J. Electrochem. Soc. 162 (2015) A2551–A2566, https://doi.org/10.1149/2.0161514jes.

[85] S. Kitajima, M. Matsuda, M. Yamato, Y. Tominaga, Anisotropic ionic conduction in composite polymer electrolytes filled with clays oriented by a strong magnetic field, Polym. J. 45 (2013) 738–743, https://doi.org/10.1038/pj.2012.207.

[86] W. Liu, S.W. Lee, D. Lin, F. Shi, S. Wang, A.D. Sendek, Y. Cui, Enhancing ionic conductivity in composite polymer electrolytes with well-aligned ceramic nanowires, Nat. Energy 2 (2017), https://doi.org/10.1038/nenergy.2017.35.

[87] J. Wan, J. Song, Z. Yang, D. Kirsch, C. Jia, R. Xu, J. Dai, M. Zhu, L. Xu, C. Chen, Y. Wang, Y. Wang, E. Hitz, S.D. Lacey, Y. Li, B. Yang, L. Hu, Highly anisotropic conductors, Adv. Mater. 29 (2017), https://doi.org/10.1002/adma.201703331.

[88] J. Billaud, F. Bouville, T. Magrini, C. Villevieille, A.R. Studart, Magnetically aligned graphite electrodes for high-rate performance Li-ion batteries, Nat. Energy 1 (2016) 1–6, https://doi.org/10.1038/NENERGY.2016.97.

[89] J.S. Sander, R.M. Erb, L. Li, A. Gurijala, Y.M. Chiang, High-performance battery electrodes via magnetic templating, Nat. Energy 1 (2016), https://doi.org/10.1038/nenergy.2016.99.

[90] X. Zhang, J. Xie, F. Shi, D. Lin, Y. Liu, W. Liu, A. Pei, Y. Gong, H. Wang, K. Liu, Y. Xiang, Y. Cui, Vertically aligned and continuous nanoscale ceramic-polymer interfaces in composite solid polymer electrolytes for enhanced ionic conductivity, Nano Lett. 18 (2018) 3829–3838, https://doi.org/10.1021/acs.nanolett.8b01111.

[91] H. Zhai, P. Xu, M. Ning, Q. Cheng, J. Mandal, Y. Yang, A flexible solid composite electrolyte with vertically aligned and connected ion-conducting nanoparticles for lithium batteries, Nano Lett. 17 (2017) 3182–3187, https://doi.org/10.1021/acs.nanolett.7b00715.

[92] X. Liu, S. Peng, S. Gao, Y. Cao, Q. You, L. Zhou, Y. Jin, Z. Liu, J. Liu, Electric-field-directed parallel alignment architecting 3d lithium-ion pathways within solid composite electrolyte, ACS Appl. Mater. Interfaces 10 (2018) 15691–15696, https://doi.org/10.1021/acsami.8b01631.

[93] J. Evans, C.A. Vincent, P.G. Bruce, Electrochemical measurement of transference numbers in polymer electrolytes, Polymer 28 (1987) 2324–2328. https://doi.org/10.1016/0032-3861(87)90394-6.

[94] J. Xi, X. Tang, Enhanced lithium ion transference number and ionic conductivity of composite polymer electrolyte doped with organic–inorganic hybrid P123@SBA-15, Chem. Phys. Lett. 400 (2004) 68–73. https://doi.org/10.1016/j.cplett.2004.10.094.

[95] C.A. Angell, C. Liu, E. Sanchez, Rubbery solid electrolytes with dominant cationic transport and high ambient conductivity, Nature 362 (1993) 137. https://doi.org/10.1038/362137a0.

[96] M. Doyle, J. Newman, Analysis of transference number measurements based on the potentiostatic polarization of solid polymer electrolytes, J. Electrochem. Soc. 142 (1995) 3465–3468, https://doi.org/10.1149/1.2050005.

[97] S.H. Chung, Y. Wang, L. Persi, F. Croce, S.G. Greenbaum, B. Scrosati, E. Plichta, Enhancement of ion transport in polymer electrolytes by addition of nanoscale inorganic oxides, J. Power Sources 97 (98) (2001) 644–648. https://doi.org/10.1016/S0378-7753(01)00748-0.

[98] S.O. Tung, S. Ho, M. Yang, R. Zhang, N.A. Kotov, A dendrite-suppressing composite ion conductor from aramid nanofibres, Nat. Commun. 6 (2015), https://doi.org/10.1038/ncomms7152.

[99] M.D. Tikekar, S. Choudhury, Z. Tu, L.A. Archer, Design principles for electrolytes and interfaces for stable lithium-metal batteries, Nat. Energy (2016), https://doi.org/10.1038/nenergy.2016.114.

[100] C. Monroe, J. Newman, The impact of elastic deformation on deposition kinetics at lithium/polymer interfaces, J. Electrochem. Soc. 152 (2005) A396, https://doi.org/10.1149/1.1850854.

[101] O. Sheng, C. Jin, J. Luo, H. Yuan, H. Huang, Y. Gan, J. Zhang, Y. Xia, C. Liang, W. Zhang, X. Tao, Mg2B2O5 nanowire enabled multifunctional solid-state electrolytes with high ionic conductivity, excellent mechanical properties, and flame-retardant performance, Nano Lett. 18 (2018) 3104–3112, https://doi.org/10.1021/acs.nanolett.8b00659.

[102] F. Capuano, F. Croce, B. Scrosati, Composite polymer electrolytes, J. Electrochem. Soc. 138 (1991) 1918–1922, https://doi.org/10.1149/1.2085900.

[103] W. Gang, J. Roos, D. Brinkmann, F. Capuano, F. Croce, B. Scrosati, Comparison of NMR and conductivity in (PEP)8LiClO4+γ-LiAlO2, Solid State Ionics 53 (56) (1992) 1102–1105, https://doi.org/10.1016/0167-2738(92)90297-3.

[104] F. Croce, R. Curini, A. Martinelli, L. Persi, F. Ronci, B. Scrosati, R. Caminiti, Physical and chemical properties of nanocomposite polymer electrolytes, J. Phys. Chem. B 103 (1999) 10632–10638, https://doi.org/10.1021/jp992307u.

[105] S.A. Khan, G.L. Baker, S. Colson, Composite polymer electrolytes using fumed silica fillers: rheology and ionic conductivity, Chem. Mater. 6 (1994) 2359–2363, https://doi.org/10.1021/cm00048a023.

[106] J. Fan, S.R. Raghavan, X.Y. Yu, S.A. Khan, P.S. Fedkiw, J. Hou, G.L. Baker, Composite polymer electrolytes using surface-modified fumed silicas: Conductivity and rheology, Eur. Coat. J. 3 (2001) 98–105, https://doi.org/10.1016/S0167-2738(98)00151-9.

[107] S. Choudhury, R. Mangal, A. Agrawal, L.A. Archer, A highly reversible room-temperature lithium metal battery based on crosslinked hairy nanoparticles, Nat. Commun. 6 (2015), https://doi.org/10.1038/ncomms10101.

[108] Y. Lu, M. Tikekar, R. Mohanty, K. Hendrickson, L. Ma, L.A. Archer, Stable cycling of lithium metal batteries using high transference number electrolytes, Adv. Energy Mater. 5 (2015), https://doi.org/10.1002/aenm.201402073.

[109] Z. Cai, Y. Liu, S. Liu, L. Li, Y. Zhang, High performance of lithium-ion polymer battery based on non-aqueous lithiated perfluorinated sulfonic ion-exchange membranes, Energy Environ. Sci. 5 (2012) 5690–5693, https://doi.org/10.1039/c1ee02708e.

[110] J. Lopez, Y. Sun, D.G. Mackanic, M. Lee, A.M. Foudeh, M.-S. Song, Y. Cui, Z. Bao, A dual-crosslinking design for resilient lithium-ion conductors, Adv. Mater. 0 (2018) 1804142, https://doi.org/10.1002/adma.201804142.

[111] J.B. Goodenough, Y. Kim, Challenges for rechargeable batteries, J. Power Sources 196 (2011) 6688–6694, https://doi.org/10.1016/j.jpowsour.2010.11.074.

[112] B.C. Melot, J.M. Tarascon, Design and preparation of materials for advanced electrochemical storage, Acc. Chem. Res. 46 (2013) 1226–1238, https://doi.org/10.1021/ar300088q.

[113] M.R. Palacín, A. De Guibert, Batteries: Why do batteries fail? Science 351 (2016) https://doi.org/10.1126/science.1253292.

[114] J. Ma, Z. Liu, B. Chen, L. Wang, L. Yue, H. Liu, J. Zhang, Z. Liu, G. Cui, A strategy to make high voltage licoo $_2$ compatible with polyethylene oxide electrolyte in all-solid-state lithium ion batteries, J. Electrochem. Soc. 164 (2017) A3454–A3461, https://doi.org/10.1149/2.0221714jes.

[115] W. Xu, J. Belieres, C.A. Angell, Ionic conductivity and electrochemical stability of Poly[oligo(ethylene glycol) oxalate] -lithium salt complexes, Chem. Mater. 13 (2001) 575–580, https://doi.org/10.1021/cm000694a.

[116] Z. Xue, D. He, X. Xie, Poly(ethylene oxide)-based electrolytes for lithium-ion batteries, J. Mater. Chem. 3 (2015) 19218–19253, https://doi.org/10.1039/c5ta03471j.

[117] W.D. Richards, L.J. Miara, Y. Wang, J.C. Kim, G. Ceder, Interface stability in solid-state batteries, Chem. Mater. 28 (2016) 266–273, https://doi.org/10.1021/acs.chemmater.5b04082.

[118] Y. Inaguma, Lithium ion conductivity in the perovskite-type LiTaO3-SrTiO3 solid solution, Solid State Ionics 79 (1995) 91–97, https://doi.org/10.1016/0167-2738(95)00036-6.

[119] C.H. Chen, K. Amine, Ionic conductivity, lithium insertion and extraction of lanthanum lithium titanate, Solid State Ionics 144 (2001) 51–57, https://doi.org/10.1016/S0167-2738(01)00884-0.

[120] Y. Li, W. Zhou, X. Chen, X. Lü, Z. Cui, S. Xin, L. Xue, Q. Jia, J.B. Goodenough, Mastering the interface for advanced all-solid-state lithium rechargeable batteries, Proc. Natl. Acad. Sci. Unit. States Am. 113 (2016) 13313–13317, https://doi.org/10.1073/pnas.1615912113.

[121] T. Thompson, S. Yu, L. Williams, R.D. Schmidt, R. Garcia-Mendez, J. Wolfenstine, J.L. Allen, E. Kioupakis, D.J. Siegel, J. Sakamoto, Electrochemical Window of the Li-Ion Solid Electrolyte Li7La3Zr2O12, ACS Energy Letters 2 (2017) 462–468, https://doi.org/10.1021/acsenergylett.6b00593.

[122] K. Liu, Y. Liu, D. Lin, A. Pei, Y. Cui, Materials for lithium-ion battery safety, Sci. Adv. 4 (2018), https://doi.org/10.1126/sciadv.aas9820.

[123] H. Akashi, K. Sekai, K.I. Tanaka, A novel fire-retardant polyacrylonitrile-based gel electrolyte for lithium batteries, Electrochim. Acta 43 (1998) 1193–1197, https://doi.org/10.1016/S0013-4686(97)10019-6.

[124] D.H.C. Wong, J.L. Thelen, Y. Fu, D. Devaux, A.A. Pandya, V.S. Battaglia, N.P. Balsara, J.M. DeSimone, Nonflammable perfluoropolyether-based

electrolytes for lithium batteries, Proc. Natl. Acad. Sci. Unit. States Am. 111 (2014) 3327–3331, https://doi.org/10.1073/pnas.1314615111.
[125] A. Agrawal, S. Choudhury, L.A. Archer, A highly conductive, non-flammable polymer-nanoparticle hybrid electrolyte, RSC Adv. 5 (2015) 20800–20809, https://doi.org/10.1039/c5ra01031d.
[126] K. Liu, W. Liu, Y. Qiu, B. Kong, Y. Sun, Z. Chen, D. Zhuo, D. Lin, Y. Cui, Electrospun core-shell microfiber separator with thermal-triggered flame-retardant properties for lithium-ion batteries, Sci. Adv. 3 (2017), https://doi.org/10.1126/sciadv.1601978.
[127] J. Wan, W. Bao, Y. Liu, J. Dai, F. Shen, L. Zhou, X. Cai, D. Urban, Y. Li, K. Jungjohann, M.S. Fuhrer, L. Hu, In Situ Investigations of Li-MoS 2 with Planar Batteries, Adv. Energy Mater. (2014) 1–7, https://doi.org/10.1002/aenm.201401742, 1401742.
[128] J.L. Shui, J.S. Okasinski, P. Kenesei, H.A. Dobbs, D. Zhao, J.D. Almer, D.J. Liu, Reversibility of anodic lithium in rechargeable lithium-oxygen batteries, Nat. Commun. 4 (2013), https://doi.org/10.1038/ncomms3255.
[129] P. Lightfoot, M.A. Mehta, P.G. Bruce, Crystal structure of the polymer electrolyte poly(ethylene oxide)3LiCF3SO3, Science 262 (1993) 883–885.
[130] M. Marzantowicz, J.R. Dygas, F. Krok, Z. Florjańczyk, E. Zygadło-Monikowska, Influence of crystallization on dielectric properties of PEO:LiTFSI polymer electrolyte, J. Non-Cryst. Solids 352 (2006) 5216–5223, https://doi.org/10.1016/j.jnoncrysol.2006.02.161.
[131] M. Marzantowicz, J.R. Dygas, F. Krok, J.L. Nowiński, A. Tomaszewska, Z. Florjańczyk, E. Zygadło-Monikowska, Crystalline phases, morphology and conductivity of PEO:LiTFSI electrolytes in the eutectic region, J. Power Sources 159 (2006) 420–430, https://doi.org/10.1016/j.jpowsour.2006.02.044.
[132] L. Edman, Ion association and ion solvation effects at the crystalline–amorphous phase transition in PEO–LiTFSI, J. Phys. Chem. B 104 (2000) 7254–7258, https://doi.org/10.1021/jp000082d.
[133] I. Rey, P. Johansson, J. Lindgren, J.C. Lassègues, J. Grondin, L. Servant, Spectroscopic and theoretical study of (CF3SO2)2N(TFSI-) and (CF3SO2) 2NH(HTFSI), J. Phys. Chem. 102 (1998) 3249–3258, https://doi.org/10.1021/jp980375v.
[134] I. Rey, J.C. Lassègues, J. Grondin, L. Servant, Infrared and Raman study of the PEO-LiTFSI polymer electrolyte, Electrochim. Acta 43 (1998) 1505–1510, https://doi.org/10.1016/S0013-4686(97)10092-5.
[135] S.J. Wen, T.J. Richardson, D.I. Ghantous, K. a Striebel, P.N. Ross, E.J. Cairns, FTIR characterization of PEO+LiN(CF3SO2)(2) electrolytes, J. Electroanal. Chem. 408 (1996) 113–118, https://doi.org/10.1016/0022-0728(96)04536-6.
[136] X. Zhang, T. Liu, S. Zhang, X. Huang, B. Xu, Y. Lin, B. Xu, L. Li, C.W. Nan, Y. Shen, Synergistic coupling between Li6.75La3Zr175Ta0.25O12and poly(-vinylidene fluoride) induces high ionic conductivity, mechanical strength, and thermal stability of solid composite electrolytes, J. Am. Chem. Soc. 139 (2017) 13779–13785, https://doi.org/10.1021/jacs.7b06364.
[137] Y. Gong, Y. Chen, Q. Zhang, F. Meng, J.-A. Shi, X. Liu, X. Liu, J. Zhang, H. Wang, J. Wang, Q. Yu, Z. Zhang, Q. Xu, R. Xiao, Y.-S. Hu, L. Gu, H. Li, X. Huang, L. Chen, Three-dimensional atomic-scale observation of structural evolution of cathode material in a working all-solid-state battery, Nat. Commun. 9 (2018) 3341, https://doi.org/10.1038/s41467-018-05833-x.
[138] J. Wan, F. Shen, W. Luo, L. Zhou, J. Dai, X. Han, W. Bao, Y. Xu, J. Panagiotopoulos, X. Fan, D. Urban, A. Nie, R. Shahbazian-Yassar, L. Hu, In situ transmission electron microscopy observation of sodiation-desodiation in a long cycle, high-capacity reduced graphene oxide sodium-ion battery anode, Chem. Mater. 28 (2016), https://doi.org/10.1021/acs.chemmater.6b01959.
[139] J.Y. Huang, L. Zhong, C.M. Wang, J.P. Sullivan, W. Xu, L.Q. Zhang, S.X. Mao, N.S. Hudak, X.H. Liu, A. Subramanian, H. Fan, L. Qi, A. Kushima, J. Li, In situ observation of the electrochemical lithiation of a single SnO2nanowire electrode, Science 330 (2010) 1515–1520, https://doi.org/10.1126/science.1195628.
[140] Y. Yuan, K. Amine, J. Lu, R. Shahbazian-Yassar, Understanding materials challenges for rechargeable ion batteries with in situ transmission electron microscopy, Nat. Commun. 8 (2017), https://doi.org/10.1038/ncomms15806.
[141] Z. Li, X. Tan, P. Li, P. Kalisvaart, M.T. Janish, W.M. Mook, E.J. Luber, K.L. Jungjohann, C.B. Carter, D. Mitlin, Coupling in situ TEM and ex situ analysis to understand heterogeneous sodiation of antimony, Nano Lett. 15 (2015) 6339–6347, https://doi.org/10.1021/acs.nanolett.5b03373.
[142] J. Zheng, M. Tang, Y.Y. Hu, Lithium ion pathway within Li7La3Zr2O12-polyethylene oxide composite electrolytes, Angew. Chem. Int. Ed. 55 (2016) 12538–12542, https://doi.org/10.1002/anie.201607539.
[143] K.J. Harry, D.T. Hallinan, D.Y. Parkinson, A.A. MacDowell, N.P. Balsara, Detection of subsurface structures underneath dendrites formed on cycled lithium metal electrodes, Nat. Mater. 13 (2014) 69–73, https://doi.org/10.1038/nmat3793.
[144] C. Wang, Y. Gong, J. Dai, L. Zhang, H. Xie, G. Pastel, B. Liu, E. Wachsman, H. Wang, L. Hu, In situ neutron depth profiling of lithium metal-garnet interfaces for solid state batteries, J. Am. Chem. Soc. 139 (2017) 14257–14264, https://doi.org/10.1021/jacs.7b07904.
[145] J. Zheng, Y.Y. Hu, New insights into the compositional dependence of li-ion transport in polymer-ceramic composite electrolytes, ACS Appl. Mater. Interfaces 10 (2018) 4113–4120, https://doi.org/10.1021/acsami.7b17301.
[146] A. Chiappone, S. Jeremias, R. Bongiovanni, M. Schönhoff, NMR study of photo-crosslinked solid polymer electrolytes: The influence of monofunctional oligoethers, J. Polym. Sci. B Polym. Phys. 51 (2013) 1571–1580, https://doi.org/10.1002/polb.23371.
[147] D.G. Mackanic, W. Michaels, M. Lee, D. Feng, J. Lopez, J. Qin, Y. Cui, Z. Bao, Crosslinked poly(tetrahydrofuran) as a loosely coordinating polymer electrolyte, Adv. Energy Mater. 0 (2018) 1800703, https://doi.org/10.1002/aenm.201800703.
[148] S. Chandrashekar, N.M. Trease, H.J. Chang, L.S. Du, C.P. Grey, A. Jerschow, 7Li MRI of Li batteries reveals location of microstructural lithium, Nat. Mater. 11 (2012) 311–315, https://doi.org/10.1038/nmat3246.
[149] R. Bhattacharyya, B. Key, H. Chen, A.S. Best, A.F. Hollenkamp, C.P. Grey, In situ NMR observation of the formation of metallic lithium microstructures in lithium batteries, Nat. Mater. 9 (2010) 504–510, https://doi.org/10.1038/nmat2764.
[150] F. Shi, A. Pei, A. Vailionis, J. Xie, B. Liu, J. Zhao, Y. Gong, Y. Cui, Strong texturing of lithium metal in batteries, Proc. Natl. Acad. Sci. Unit. States Am. 114 (2017) 12138–12143, https://doi.org/10.1073/pnas.1708224114.
[151] L. Gireaud, S. Grugeon, S. Laruelle, B. Yrieix, J.M. Tarascon, Lithium metal stripping/plating mechanisms studies: A metallurgical approach, Electrochem. Commun. 8 (2006) 1639–1649, https://doi.org/10.1016/j.elecom.2006.07.037.
[152] C. Brissot, M. Rosso, J.N. Chazalviel, S. Lascaud, In situ concentration cartography in the neighborhood of dendrites growing in lithium/polymer-electrolyte/lithium cells, J. Electrochem. Soc. 146 (1999) 4393–4400, https://doi.org/10.1149/1.1392649.
[153] X. Yao, N. Huang, F. Han, Q. Zhang, H. Wan, J.P. Mwizerwa, C. Wang, X. Xu, High-performance all-solid-state lithium–sulfur batteries enabled by amorphous sulfur-coated reduced graphene oxide cathodes, Adv. Energy Mater. 7 (2017), https://doi.org/10.1002/aenm.201602923.
[154] B.D. McCloskey, Attainable gravimetric and volumetric energy density of li-s and li ion battery cells - supp info, J. Phys. Chem. Lett. 6 (2015) 4581–4588, https://doi.org/10.1021/acs.jpclett.5b01814.
[155] J. Płocharski, W. Weiczorek, PEO based composite solid electrolyte containing nasicon, Solid State Ionics (1988), https://doi.org/10.1016/0167-2738(88)90315-3.